Pacific Gas and Electric Company®

James R. Becker
Site Vice President

Diablo Canyon Power Plant
Mail Code 104/5/601
P. O. Box 56
Avila Beach, CA 93424

805.545.3462
Internal: 691.3462
Fax: 805.545.6445

February 26, 2010

PG&E Letter No. DCL-10-019

U.S. Nuclear Regulatory Commission
ATTN: Document Control Desk
Washington, DC 20555-0001

Docket No. 50-275, OL-DPR-80
Docket No. 50-323, OL-DPR-82
Diablo Canyon Units 1 and 2
Requested Documents From The NRC - PG&E Shoreline Fault Zone Meeting

Dear Commissioners and Staff:

On January 5, 2010, representatives from Pacific Gas and Electric Company (PG&E) met with the NRC to discuss the analysis of the California Central Coast Shoreline Fault Zone that is in close proximity to the Diablo Canyon Power Plant (DCPP).

During this meeting PG&E agreed to provide the following for the NRC staff:

- Calculation: Evaluation of Secondary Fault Rupture Hazard From The Shoreline Fault Zone
- A copy of a paper by Lloyd Cluff dated 1985 regarding techniques for assessment of fault activity slip rates

Enclosure 1 and 2 provide the above requested documents. Enclosure 2 supports the previously communicated conclusion that secondary deformation due to the shoreline fault zone results in negligible change in the DCPP seismic core damage frequency.

PG&E makes no regulatory commitments as a part of this submittal.

Sincerely,

James R. Becker

swh/50086062/018

A001
NRR

Enclosures
cc: Norman A. Abrahamson
Lloyd S. Cluff
Elmo C. Collins, NRC Region IV
Annie M. Kammerer, NRC
Marcia K. McLaren
Michael S. Peck, DCPP NRC Resident
Alan B. Wang, NRR

Enclosure 1
PG&E Letter DCL-10-019

Evaluation of Secondary Fault Rupture Hazard From The Shoreline Fault Zone

PACIFIC GAS AND ELECTRIC COMPANY
GEOSCIENCES DEPARTMENT
CALCULATION DOCUMENT

Calc Number: GEO.DCPP.10.01
Calc Revision: 0
Calc Date: 02/25/10
Quality related: Y
ITR Verification method: B

1. **CALCULATION TITLE:** Evaluation of secondary fault rupture hazard from the Shoreline fault zone.

2. **SIGNATORIES:**

PREPARED BY: _____ DATE: 02/25/2010
Kathryn Wooddell — Printed Name
Geosciences — Organization

VERIFIED BY: _____ DATE: 2/25/2010
Nick Gregor — Printed Name
Consultant — Organization

APPROVED BY: _____ DATE: 2/25/2010
Lloyd Cluff — Printed Name
Geosciences — Organization

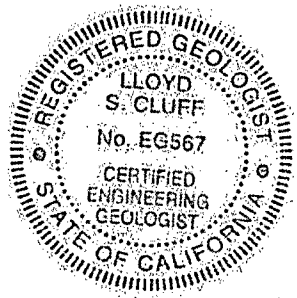

Exp 9/30/2011

3. RECORD OF REVISIONS:

Rev. No.	Reason for Revision	Revision Date
0	Initial Calc. Reference: Notification 50086062 Task 12	02/25/10

4. PURPOSE:

The Shoreline fault zone is being characterized as part of a two-year study that will be completed in December 2010. During the first year of the study, an offshore fault that may be the surface expression of the Shoreline fault zone was identified through offshore geophysical surveys. This fault is located 0.6 km from the DCPP power block. Additional work during 2010 is needed to complete the characterization of the Shoreline fault zone and, in particular, to constrain the activity rate of the fault; however, given that the distance to the identified offshore fault is less than 1 km, the potential for secondary rupture, on the order of a few cm, is considered. The only safety related structures that would be impacted by small secondary displacements resulting from the secondary fault rupture are eight Dresser couplings along the Auxiliary Salt Water (ASW) pipes that are located in the weaker rock unit called Unit c of the Obispo Formation (Tof_c) (PG&E, 2009). Per Notification 50086062 Task 12, the purpose of this calculation is to estimate the probability that secondary surface rupture will occur at any one of the eight Dresser couplings along the ASW pipes from an earthquake along the Shoreline fault zone.

5. ASSUMPTIONS:

5.1. STYLE OF FAULTING

It is assumed that the Shoreline fault zone is a strike-slip feature. The basis for this assumption is the characterization in the Action Plan that describes the Shoreline fault zone as a vertical strike-slip fault zone.

5.2. SEISMOGENIC THICKNESS

A seismogenic thickness of 12 kilometers is assumed for the Central and Southern sections of the Shoreline fault zone. The basis for this assumption is that it is the thickness of the other faults in the region (LTSP, PGE 1988)

5.3. MINIMUM EARTHQUAKE MAGNITUDE FOR MOMENT BALANCE (Mm=0)

It is assumed that the minimum earthquake magnitude for balancing moment on the fault is magnitude 0. The basis for this assumption is that it is a commonly assumed value for calculating the activity rate based on moment balancing used in seismic hazard studies.

5.4. MINIMUM EARTHQUAKE MAGNITUDE FOR FAULT RUPTURE (Mmin)

It is assumed that the minimum earthquake magnitude for fault rupture is M5.0. The basis for this assumption is that, given a model fit to the empirical data in Wells and Coppersmith (1994), no surface rupture is expected on a fault for earthquakes below M5.0.

5.5. FAULT b-VALUE

It is assumed that the b-value for the Shoreline fault zone is 0.8. This assumption is based on the average b-value for California published by the USGS.

5.6. SHEAR MODULUS OF THE CRUST

The shear modulus of the crust is assumed to be 3.0e11 dyne/cm^2. This is a commonly assumed value for this parameter.

5.7. YOUNGS AND COPPERSMITH CHARACTERISTIC EARTHQUAKE MODEL

The Youngs and Coppersmith (1985) characteristic earthquake model is commonly assumed to represent the best model for describing the magnitude-frequency distribution of earthquakes on a fault.

5.8. WELLS AND COPPERSMITH RELATION FOR MAXIMUM DISPLACEMENT GIVEN MAGNITUDE

The Wells and Coppersmith (1994) relationship for maximum displacement given magnitude is used to calculate the mean maximum displacement in meters given a moment magnitude. The basis for this assumption is that this relationship represents the state of the practice.

5.9. PRIMARY FAULT RUPTURE

This calculation assumes uniform rupture of the Shoreline fault zone along the entire rupture area. It is therefore assumed that the primary surface rupture includes the section of the fault closest to DCPP. This is a conservative assumption made to simplify the calculation.

5.10. PROBABILITY OF SECONDARY FAULT RUPTURE

The probability of secondary fault rupture within a 50 m x 50 m zone is assumed to follow the lower range of the Petersen et al (2004) data set as shown by the curve in Figure 5-1. The basis for this assumption is that the Shoreline fault zone is a straight strike-slip fault zone in the region offshore DCPP (PG&E, 2010), whereas, the data used by Petersen et al (2004) included secondary ruptures from strike-slip faults with more complex traces and stepovers.

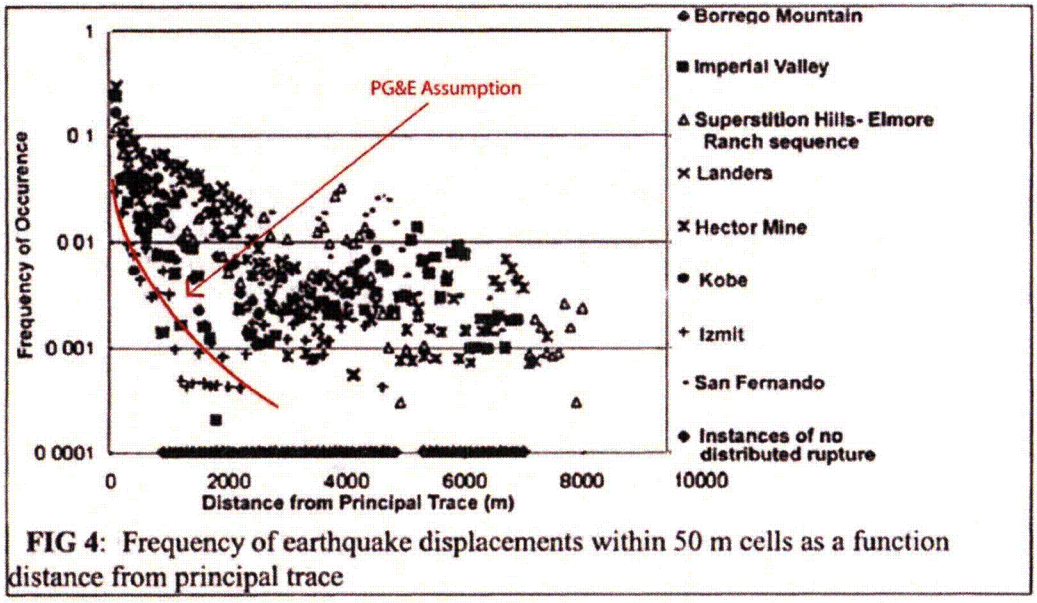

Figure 5-1. Frequency of earthquake displacements within 50 m cells as a function of distance from principal trace (Petersen et al, 2004). The red line shows the PG&E assumption.

5.11. GEOMETRY OF SECONDARY SURFACE RUPTURES

- It is assumed that if there is secondary rupture within the 50 m x 50 m zone that contains one or more of the Dresser Couplings, the secondary rupture will have a length that covers the full 50 m width of the zone. The basis for this assumption is that many secondary ruptures observed in past earthquakes have lengths of 50 m or more and it is conservative in terms of the hazard.

- It is also assumed that the secondary rupture is concentrated into a single knife edge rupture within the zone. The basis for this assumption is that it is consistent with the engineering analysis of the capacity of the Dresser couplings and is conservative in terms of the potential damage to the Dresser couplings (PG&E, 2009).

5.12. ASPECT RATIO OF STRIKE SLIP FAULTS

It is assumed that all ruptures on the Shoreline fault have an aspect ratio of 1.2 based on the fault dimension (14km/12km). Typical strike-slip faults have an aspect ratio of 2, but the aspect ratio, in this case, is limited by the fault dimension.

6. INPUTS:

6.1. FAULT SEGMENTATION:

Segment	LENGTH (km)	SOURCE
Central	8	PG&E, 2010, Section 6.1 p.16
Central & Southern	14	PG&E, 2010, Section 6.1 p.16

6.2. SEISMOGENIC THICKNESS

Segment	SEISMOGENIC THICKNESS (km)	SOURCE
Central	10	PG&E, 2010, Section 4.2 p.10
Central & Southern	12	Assumption 5.2

6.3. CHARACTERISTIC MAGNITUDE

Segment	CHARACTERISTIC MAGNITUDE (M_w)	SOURCE
Central	6.00	PG&E, 2010, Section 5.2 p. 14
Central & Southern	6.25	PG&E, 2010, Section 5.2 p.14

6.4. FAULT DIP

FAULT DIP (degrees)	SOURCE
90	PG&E, 2010, Table 1 p.13

6.5. DISTANCE TO DCPP

RUPTURE DIST. (km)	SOURCE
0.6	PG&E, 2010, Section 4.3 p.10 (Distance from Shoreline fault to DCPP power block)

6.6. SHORELINE FAULT b-VALUE:

b-VALUE	SOURCE
0.8	Assumption 5.5

6.7. SHEAR MODULUS OF THE CRUST (μ):

μ (dyne/cm^2)	SOURCE
3.0e11	Assumption 5.6

6.8. SLIP RATE (S):

	S (mm/yr)	SOURCE
Lower bound	0.01	PG&E, 2010, Section 4.4 p.11, 12
Upper bound	0.3	PG&E, 2010 Section 4.4 p.12

7. METHOD AND EQUATION SUMMARY:

7.1 METHODOLOGY:

The calculation of secondary rupture hazard follows the probabilistic method of Petersen et al. (2004). In this method, the probability of a displacement d that is larger than d_0 occurring at a site location (x,y) with a square footprint that is z by z is given by Equation 2 of Petersen et al. (2004):

$$\lambda(d \geq d_0)_{XYZ} = \alpha \int_m f_M(m) \int_s f_S(s) \int_r f_R(r) P[sr \neq 0 \mid m] P[d \neq 0 \mid l,r,m,z,s,sr \neq 0] P[d \geq d_0 \mid l,r,m,d \neq 0] dr ds dm \qquad (7\text{–}1)$$

The individual terms are described below:

- **$f_M(m)$:** a probability density function that describes the magnitude-frequency distribution along a fault. Based on Assumption 5.7, the Youngs and Coppersmith (1985) characteristic model is used for $f_M(m)$.
- **α:** a rate parameter that describes how often the earthquakes occur in the model above some minimum magnitude. This parameter is commonly called the activity rate, and it is defined based on a moment balance of the total accumulated seismic moment over the mean moment released per earthquake.
- **$f_S(s)$:** a probability density function that describes the probability of a rupture at a specific place along a fault. Based on Assumption 5-9, the fault rupture always passes through the point on the fault plane nearest to DCPP.
- **$P[sr \neq 0 \mid m]$:** the probability of surface rupture given magnitude. This probability term accounts for the possibility that an earthquake rupture on a fault will not reach the surface.
- **$P[d \neq 0 \mid l,r,m,z,s,sr \neq 0]$:** the probability of having non-zero displacement at a location (l, r) for a foundation size z given magnitude and an event with surface rupture.
- **$P[d \geq d_0 \mid l,r,m,d \neq 0]$:** the probability of the secondary displacement d greater than or equal to a given value d_0 at a location (l, r) given the magnitude of the earthquake on the Shoreline fault zone.
- **$f_R(r)$:** a probability density function to define the distance from the main fault rupture to the site.

Based on Assumption 5.9, if there is surface rupture, it is assumed that the surface rupture includes the section of the fault closest to DCPP. With this assumption, the $P[sr \neq 0]$ terms are not dependent on location of the rupture (s). In addition, the closest distance from the rupture to the site is a constant (r_{min}), so f(r) becomes a delta function. Equation (7-1) becomes:

$$\lambda(d \geq d_0) = \alpha \int_{m=M_{min}}^{M_{max}} f_m(M) \int_S f_S(s) ds \int_r \delta(r - r_{min}) P[sr \neq 0 | M, s] P[d \neq 0 | r, z, sr \neq 0] \\ P[d \geq d_0 | M, d \neq 0] dM\, dr \quad (7\text{–}2)$$

Equation (7-2) simplifies to the following:

$$\lambda(d \geq d_0) = \alpha \int_{m=M_{min}}^{M_{max}} f_m(M) P[sr \neq 0 | M] P[d \neq 0 | r_{min}, z, sr \neq 0] P[d \geq d_0 | M, d \neq 0] dM \quad (7\text{–}3)$$

The Petersen et al (2004) paper gives a model for the probability of secondary rupture occurring within a 50 m x 50 m region at a distance r from the main trace. For this application, the area for the eight Dresser couplings is smaller than 50m x 50 m. The $P[d\neq0|r_{min},z,sr\neq0]$ term can be written in terms of the probability that there is secondary rupture in a 50 m x 50 m region that contains the eight Dresser couplings and the probability that the secondary rupture is through one of the 8 Dresser couplings given that there is secondary rupture in the 50 m x 50 m region containing the Dresser couplings:

$$P[d \neq 0 | r_{min}, z, sr \neq 0] = P[d_1 \neq 0 | r_{min}, z_1 = 50m\_x\_50m, sr \neq 0] P[d \neq 0 | z, d_1 \neq 0] \quad (7\text{–}4)$$

where z is the combined area of the small region containing the eight Dresser couplings. The $P[d_1\neq0|r_{min},z_1=50m \text{ x } 50m,sr\neq0]$ term is 0.004. It is read from Figure 5-1 (Petersen et al., 2004) Based on Assumption 5-11, the secondary rupture is assumed to have a length of at least 50 m, so the $P[d\neq0|z,d_1\neq0]$ term is 0.048768 (see Section 8. Body of Calculations).

7.2 EQUATIONS

7.2.1. Youngs and Coppersmith Characteristic Earthquake Model ($f_M(m)$)

The Youngs and Coppersmith (1985) characteristic earthquake model is used to calculate the probability density function for the magnitude-frequency distribution along a fault.

for $M_{char} - 0.25 < M \leq M_{char} + 0.25$

$$f_m^{YC}(m) = \frac{1}{1 + c_2} \frac{\beta \exp(-\beta(M_{char} - M_{min} - 1.25))}{1 - \exp(-\beta(M_{char} - M_{min} - 0.25))} \quad (7\text{-}5a)$$

for $M_{min} \leq M \leq M_{char} - 0.25$

$$f_m^{YC}(m) = \frac{1}{1 + c_2} \frac{\beta \exp(-\beta(M - M_{min}))}{1 - \exp(-\beta(M_{char} - M_{min} - 0.25))} \quad (7\text{-}5b)$$

where: $c_2 = \frac{0.5\beta \exp(-\beta(M_{char} - M_{\min} - 1.25))}{1 - \exp(-\beta(M_{char} - M_{\min} - 0.25))}$ (7-6)

$\beta = \ln(10) * (b - value)$ (7-7)

7.2.2. Activity Rate (α)

The rate of earthquakes on the fault above M=0 is computed by balancing the annual rate of moment accumulation on the fault, $\dot{M}_0$, with the long term rate of moment release in earthquakes. The following equations (7-8 to 7-12) for computing the activity rate based on fault slip-rates are given in Abrahamson (2009):

$\dot{M}_0 = \alpha(M > 0)\overline{M}_0$ (7-8)

where $\overline{M}_0$ is the mean moment per event for earthquakes above M=0. The moment rate is given by:

$\dot{M}_0 = \mu AS$ (7-9)

and the mean moment per event is given by:

$\overline{M}_0(M) = \int_m f_m(M) M_0(M) dM$ (7-10)

where the moment for α is given by:

$M_0(M) = 10^{1.5m+16.05}$ (7-11)

The activity rate is found by solving equation (7-8) for α:

$\alpha(M > 0) = \frac{\dot{M}_0}{\overline{M}_0}$ (7-12)

7.2.3. Probability of Surface Rupture on the Main Trace (P[sr≠0|m])

Based on Assumption 5-4, a model fit to the empirical data in Wells and Coppersmith (1994) for the probability of surface rupture is used. This model is given by a histogram and parameterized by the following equations:

Log(RA) = -3.42 + 0.90M (7-13a)

σ=0.22 log10 units (7-13b)

For M ≥ 5.0
P[sr≠0|m] = 0.5 * (tanh(2.5 * (M - 5.9)) + 1) (7-13c)

For M < 5.0
P[sr≠0|m] = 0 (7-13d)

7.2.4. Conditional Hazard from Secondary Rupture (P[d≥d_0|m,d≠0])

The conditional hazard from secondary rupture is given by:

$$P\left[d \geq d_0 \middle| m, d \neq 0\right] = 1 - \Phi\left[\frac{\log(d_0) - \left(\log(D_{\max}(m)) + \log\left(D_S / D_{\max}\right)\right)}{\sqrt{\sigma^2_{\log D_{\max}} + \sigma^2_{\log D_S / D_{\max}}}}\right] \quad (7\text{-}14)$$

where Φ is the cumulative normal distribution.

From Wells and Coppersmith (1994), Table 2B, the median value for the MD for strike-slip earthquakes is given by:

$\log(D_{max}(m)) = -7.03 + 1.03m$ (7-15)

and the standard deviation is given by:

$$\sigma_{\log D_{\max}} = 0.34 \quad (7\text{-}16)$$

Peterson et al (2004), gives a histogram for the distribution of the ratio of the secondary displacement to the maximum displacement on the main trace (D_s/D_{max}). This histogram was digitized and a mean and standard deviation were computed:

$\log(D_S/D_{max}) = -1.587$ (7-17)

$$\sigma_{\log\left(D_S / D_{\max}\right)} = 0.537 \quad (7\text{-}18)$$

The log-normal distribution based on the parameters in equations 7-17 and 7-18 is compared to the histogram in Figure 7-1. The log-normal distribution is a reasonable approximation to the histogram.

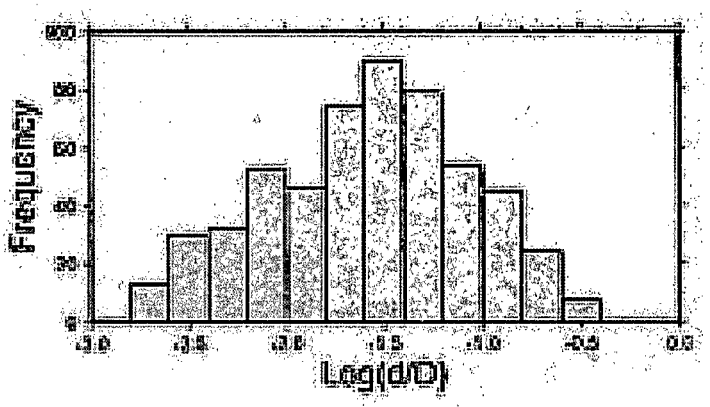

Figure 7-1. Histogram showing the frequency of log10 normalized displacements (Petersen et al., 2004)

8. SOFTWARE:

All calculations were made using a script written in MatLab v7.4.0 (R2007a). An independent verification of the MatLab script was preformed in excel. The agreement between the MatLab and Excel values indicate that MatLab is operating correctly.

9. BODY OF CALCULATIONS:

9.1 CONDITIONAL PROBABILITY OF SECONDARY RUPTURE INTERSECTING A DRESSER COUPLING

Based on Assumption 5-11, the conditional probability that rupture occurs through any one of the eight 1-ft long Dresser couplings, given that there is secondary rupture in the 50m x 50 m zone containing one or more Dresser couplings is:

$$P[d \neq 0 | z, d_1 \neq 0] = 8 \text{ ft} / 50 \text{ meters} = 2.4384 \text{ meters} / 50 \text{ meters} = 0.048768$$

9.2 CALCULATION FOR PROBABILITY OF SURFACE RUPTURE

The Wells and coppersmith (1994) data (Table 1) lists earthquakes with surface rupture and without surface rupture. The ratio of the number of earthquakes with surface rupture to the total number of earthquakes within a magnitude bin provides an estimate of the probability of surface rupture for the magnitude range. The values are listed in Table 9-1

Table 9-1. Earthquakes used by Wells & Coppersmith (1994), Table 1.

Mag Bin	Total Number of Earthquakes	Number of Earthquakes with Surface Rupture	Fraction of Earthquakes with Surface Rupture
5.0-5.5	28	3	0.107
5.5-6.0	44	14	0.318
6.0-6.5	43	20	0.465
6.5-7.0	59	45	0.763
7.0-7.5	40	35	0.875
7.5-8.0	15	14	0.933
8.0-8.5	2	2	1.000

The fraction of surface rupturing earthquakes is shown in Figure 9-1 as a function of magnitude. The Wells and Coppersmith (1994) data set is a global data set with varying crustal thickness. For the Shoreline fault, the thickness is 10 km for the central segment and 12 km for the Central & Southern Segments (Input 6.2). The widths of the two rupture scenarios restricts the magnitude for which the rupture can be buried (e.g. no surface rupture).

Using the Wells and Coppersmith (1994) model (see Table 2A) for rupture area as a function of magnitude for strike slip earthquake (Equation 7-13a),

$$\text{Log(RA)} = -3.42 + 0.90M$$

with a standard deviation of σ=0.22 log10 units.

For a given magnitude, there is a 2.5% chance of the rupture area being less than the median minus 2 σ. The 2.5th percentile rupture area as a function of magnitude is listed in Table 9-2.

$$\text{Width} = \text{sqrt(area/AspectRatio)}$$

The rupture width is the full 10 km fault width for the central segment rupture scenario for M>=6.6. The rupture width is the full 12 km width for the central & southern rupture scenario for M>=6.8. Therefore, the probability of surface rupture is 97.5% for M6.6 for the 10 km width case. Similarly, it is 97.5% for M6.8 for the 12 km width case. These two points are shown on Figure 9-1.

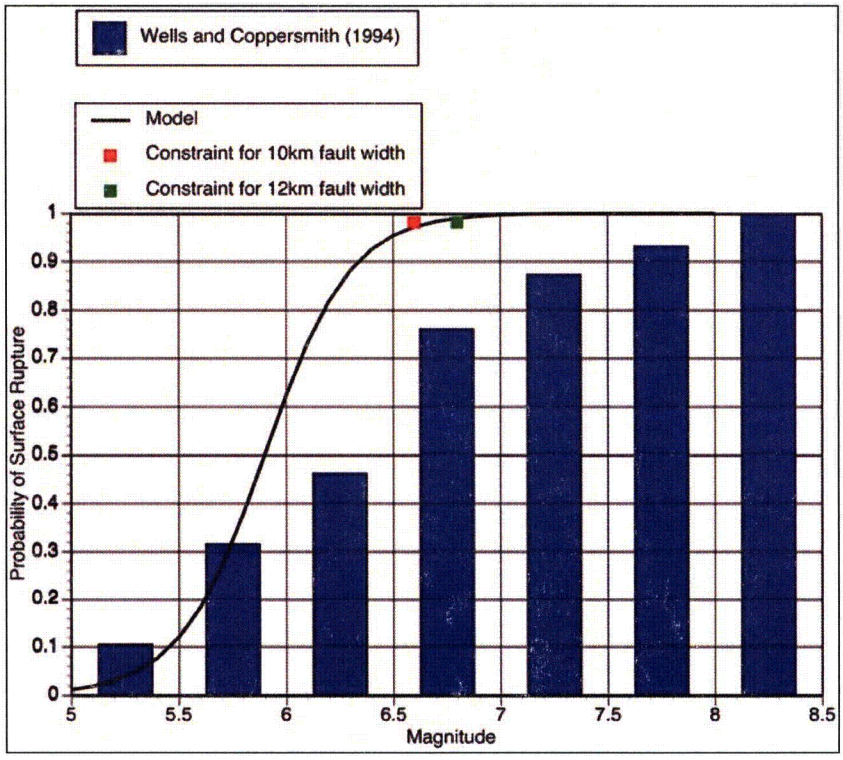

Figure 9-1. Surface Rupture Probability Histogram

Next, a smooth functional form was developed to fit the constraint on the probability of surface rupture for the two rupture scenarios for the Shoreline fault.

A hyperbolic arctangent function was used. The model parameters were selected so that the resulting probability was close to the constrained values for M6.6 to 6.8 and close to the Wells and Coppersmith values (from Table 9-1) for M5.75. The resulting fit is shown in Figure 9-1

.

For $M \geq 5.0$

$$P[sr \neq 0|m] = 0.5 * (\tanh(2.5 * (M - 5.9)) + 1) \quad (7\text{-}13c)$$

For $M < 5.0$

$$P[sr \neq 0|m] = 0 \quad (7\text{-}13d)$$

Table 9-2. 2.5th Percentile Rupture Area as a Function of Magnitude

Mag	2.5th percentile rupture area	Width for aspect ratio of 1.2
6.5	98	9.0
6.6	120	10.0
6.7	148	11.1
6.8	182	12.3
6.9	224	13.7

9.3 HAZARD CALCULATION

The MatLab computer code used to carry out the calculations is listed below:

```
%%%%%%%%%%%%%%%%%%%%%%%%%%%%%%%%%%%%%%%%%%%%%%%%%%%%%%%%%%%%%%%%%%%%%%%%%%%%%%%%
% Probabilistic Rupture Hazard:  script for calculating secondary rupture
%                                displacements
%
% Written By:  Kathryn Wooddell 12/01/2009
%              Modified         02/23/2010
%
% Note:  This script runs the case for the Central + Southern Shoreline
%        fault zone with a slip rate of 0.3mm/yr and 2.0 cm of secondary
%        rupture.  The inputs are: M6.25, L=14km, W=12km, S=0.3mm/yr, and
%        Zin=2.0cm.
%
% INPUTS FOR ALL CASES RUN IN GEO.DCPP.10.01, Rev 0:
%
% CENTRAL SEG (slip rate=0.01mm/yr and 1.0 cm of secondary rupture):
% INPUTS:  M6.0, L=8km, W=10km, S=0.01mm/yr, Zin=1.0cm
%
% CENTRAL SEG (slip rate=0.01mm/yr and 2.0 cm of secondary rupture):
% INPUTS:  M6.0, L=8km, W=10km, S=0.01mm/yr, Zin=2.0cm
%
% CENTRAL+SO SEG (slip rate=0.01mm/yr and 1.0 cm of secondary rupture):
% INPUTS:  M6.25, L=14km, W=12km, S=0.01mm/yr, Zin=1.0cm
%
% CENTRAL+SO SEG (slip rate=0.01mm/yr and 2.0 cm of secondary rupture):
% INPUTS:  M6.25, L=14km, W=12km, S=0.01mm/yr, Zin=2.0cm
%
```

```
% CENTRAL SEG (slip rate=0.3mm/yr and 1.0 cm of secondary rupture):
% INPUTS:  M6.0, L=8km, W=10km, S=0.3mm/yr, Zin=1.0cm
%
% CENTRAL SEG (slip rate=0.3mm/yr and 2.0 cm of secondary rupture):
% INPUTS:  M6.0, L=8km, W=10km, S=0.3mm/yr, Zin=2.0cm
%
% CENTRAL+SO SEG (slip rate=0.3mm/yr and 1.0 cm of secondary rupture):
% INPUTS:  M6.25, L=14km, W=2km, S=0.3mm/yr, Zin=1.0cm
%
% CENTRAL+SO SEG (slip rate=0.3mm/yr and 2.0 cm of secondary rupture):
% INPUTS:  M6.25, L=14km, W=12km, S=0.3mm/yr, Zin=2.0cm
%%%%%%%%%%%%%%%%%%%%%%%%%%%%%%%%%%%%%%%%%%%%%%%%%%%%%%%%%%%%%%%%%%%%%%%%%%%%%%%

% INPUT VALUES:
Mchar = 6.25;          % Mean char. EQ mag (2 Cases: M6.0, M6.25) (Input6.3)
Mmin = 5.0;            % Min. EQ mag for fault rupture (Assumption 5.4)
Mmo = 0.0;             % Min. EQ mag for moment balance (Assumption 5.3)
delM = 0.01;           % Magnitude increment (step size)
b = 0.8;               % Fault b-value (Assumption 5.5)
mumod = 3.00e+11;      % Shear Modulus of crust (dyne/cm^2) (Assumption 5.6)
L = 1400000;           % Fault length (cm) (2 Cases: 8km, 14km) (Input 6.1)
W = 1200000;           % Fault width (cm) (2 Cases: 10km, 12km) (Input 6.2)
S = 0.03;              % Slip rate (cm/yr) (2 Cases: 0.01mm/yr, 0.3mm/yr)
                       %(Input 6.8)
Zin = 0.02             % Minimum amount of secondary rupture (m)


% DEFINE PARAMETERS USED IN SUBSEQUENT CALCULATIONS:
B = log(10)*b;         % Equation (7-7)
                        % Note:  In MatLab log(x)==ln(x), log10(x)==log(x)

% Parameter used in Y&C characteristic EQ model: Equation (7-6)
% NOTE: c2 uses a min mag (M5.5) for the min EQ mag expected to cause
% surface rupture and c2_0 uses a min EQ mag (M0) that is used to compute
% the moment balance.
c2 = (0.5*(B)*exp(-1*B*(Mchar-Mmin-1.25)))/(1-exp(-1*B*(Mchar-Mmin-
0.25)));
c2_0 = (0.5*(B)*exp(-1*B*(Mchar-Mmo-1.25)))/(1-exp(-1*B*(Mchar-Mmo-
0.25)));

MoACC = mumod*L*W*S;    % Accumulated Seismic Moment:  Equation (7-9)

% Define mag vectors for Y&C char EQ mag calculation
M = Mmin+(delM/2):delM:Mchar+0.25;  % Mag for YC calc (for fault rupture)
M_0 = Mmo+(delM/2):delM:Mchar+0.25; % Mag for YC calc (moment balance)

%Initialize arrays for Y&C mag calcs
YC = zeros(1,length(M));
YC_0 = zeros(1,length(M_0));


% YOUNGS AND COPPERSMITH CHARACTERISTIC EQ MODEL (For moment balance)
for k = 1:length(M_0)
    M_0(k)
```

```
    Mo2(k) = 10^((1.5*M_0(k))+16.05);  %Seismic Moment: Equation (7-11)
    if M_0(k) > Mchar - 0.25;                    %Mag pdf - Y&C Char. EQ
        YC_0(k) = (1/(1+c2_0))*...               %Model: Equation (7-5a)
            ((B*exp(-1*B*(Mchar-Mmo-1.25)))/...
            (1-exp(-1*B*(Mchar-Mmo-0.25))));
    else
        YC_0(k) = (1/(1+c2_0))*...               %Mag pdf - Y&C Char. EQ
            ((B*exp(-1*B*(M_0(k)-Mmo)))/...      %Model: Equation (7-5b)
            (1-exp(-1*B*(Mchar-Mmo-0.25))));
    end
    Pm_0(k) = YC_0(k)*delM;          %Probability of Earthquake Magnitude
    MoEQ(k) = Pm_0(k)*Mo2(k);        %Seismic Moment Per EQ
end
MeanMoEQ = sum(MoEQ);    %Mean seismic moment per. EQ: Equation (7-10)
NMmo = MoACC/MeanMoEQ    %Activity Rate for EQs above M0: Equation (7-12)


% YOUNGS AND COPPERSMITH CHARACTERISTIC EQ MODEL (for fault rupture)
for i = 1:length(M)
    M(i)
    Mo(i) = 10^((1.5*M(i))+16.05);  %Seismic Moment: Equation (7-11)
    if M(i) > Mchar - 0.25;                      %Mag pdf - Y&C Char. EQ
        YC(i) = (1/(1+c2))*...                   %Model: Equation (7-5a)
            ((B*exp(-1*B*(Mchar-Mmin-1.25)))/...
            (1-exp(-1*B*(Mchar-Mmin-0.25))));
    else
        YC(i) = (1/(1+c2))*...                   %Mag pdf - Y&C Char. EQ
            ((B*exp(-1*B*(M(i)-Mmin)))/...       %Model: Equation (7-5b)
            (1-exp(-1*B*(Mchar-Mmin-0.25))));
    end
    Pm(i) = YC(i)*delM;          %Probability of Earthquake Magnitude


    % PROBABILITY OF SURFACE RUPTURE GIVEN MAGNITUDE
    if M(i) >= 5.0;
        Psurf(i) = 0.5*(tanh(2.5*(M(i)-5.9))+1);     %Equation (7-13c)
    else
        Psurf(i) = 0;                                %Equation (7-13d)
    end


    % MAXIMUM DISPLACEMENT GIVEN MAGNITUDE:
    log10Dmax(i) = -7.03 + 1.03*M(i);    %Equation (7-15)
    sigma = 0.34;                        %Equation (7-16)
    mu = log10Dmax(i);


    % RATIO OF MINIMUM TO MAXIMUM DISPLACEMENT GIVEN MAGNITUDE:
    mu2 = -1.587;                        %Equation (7-17)
    sig2 = 0.537;                        %Equation (7-18)

    logd0 = (log10(Zin));                %log of min displacement value
    denom = (sigma^2 + sig2^2)^(1/2);    %denominator of Equation (7-14)
```

```
    A = ((logd0-(mu+mu2))/denom);          %Term for calculating the cum.
                                           %norm. dist. in Equation (7-14)
                                           %(epsilon*)

    Pd(i) = 1 - normcdf(A,0,1)             %Equation (7-14)

    %PROBABILITY OF SECONDARY SURFACE RUPTURE -- for values 0.04 and
    %0.048768 see "Body of Calculations"

    %integrand of Equation (7-3)
    P1(i) = Pd(i)*Pm(i)*Psurf(i)*0.004*0.048768;
    %integrand scaled by activity rate
    Haz(i) = NMmo.*(10^((-1*b)*Mmin)).*P1(i);

end

Hazard = sum(Haz);
```

10. RESULTS AND CONCLUSIONS:

RESULTS

The results of the secondary rupture hazard are given in Table 9-1 in terms of the probability of exceeding 1 cm and 2 cm at any one of the eight Dresser couplings. This table gives the results for a range of assumptions on the segmentation of the Shoreline fault zone (Input 6-1) and on the slip-rate of the Shoreline fault zone (Input 6-8).

Table 10-1. Results of the Secondary Rupture Hazard

Segment	Slip-rate (mm/yr)	Annual Probability of Exceedance	
		1 cm	2 cm
Central	0.01	2.6e-10	1.4e-10
Central & Southern	0.01	6.0e-10	3.5e-10
Central	0.3	7.8e-9	4.1e-9
Central & Southern	0.3	1.8e-8	1.1e-8

CONCLUSIONS

The chance of secondary rupture from the nearby Shoreline fault zone damaging one of the eight Dresser couplings in the ASW pipes in the Tof_c formation is very unlikely. With the current uncertainties in the characterization of the Shoreline fault zone, the annual probability of secondary rupture of 1 to 2 cm at any of the eight Dresser couplings is between 2e-08 and 1e-10. This large uncertainty is mainly due to the large uncertainty in the slip-rate on the Shoreline fault zone.

11. LIMITATIONS:

This calculation uses a range of estimates of the slip-rate for the Shoreline fault zone that were between 0.01 and 0.3 mm/yr. This leads to the large uncertainty in the computed secondary rupture hazard. There is an ongoing study to improve the constraints on the slip-rate of the Shoreline fault zone. Although not expected, if the new slip-rate from the ongoing work is much larger than 0.3 mm/yr, then this evaluation will need to be repeated.

12. IMPACT EVALUATION:

The impacts are evaluated in terms of the increase to the seismic core damage frequency (CDF) for DCPP. The seismic CDF at DCPP is 3.7e-5 (LTSP, 1988). The chance of secondary rupture occurring at any of the eight Dresser couplings in the ASW pipes is very

unlikely: in the range of 2e-08 and 1e-10 for 1 to 2 cm of secondary rupture. Even if we assume that failure of one of the Dresser couplings lead to core damage, the increase in the seismic CDF is between 0.0001% and 0.01%. Therefore, secondary rupture hazard has a negligible impact on the seismic CDF for DCPP.

13. REFERENCES:

Abrahamson, Norman (2009). UC Berkeley Class Notes: Chapter 6.

Pacific Gas and Electric Company (1988). Final Report of the Diablo Canyon Long-Term-Seismic Program: U.S. Nuclear Regulatory Commission Docket Nos. 50-275 and 50-323.

Pacific Gas and Electric Company (2009). Calculation 17-107,Rev 0, Postulated ground deformation shoreline fault auxiliary salt water buried piping stress analysis, August 3, 2009.

Pacific Gas and Electric Company (2010). Progress Report: Shoreline fault zone, central coastal California: U.S. Nuclear Regulatory Commission Docket Nos. 50-275 and 50-323, PG&E Letter No. DCL-10-003, January 13, 2010.

Petersen, M., Tianqing, C., Dawson, T., Frankel, A., Wills, C., and Schwartz, D. (2004). Evaluating fault rupture hazard for strike-slip earthquakes, Geotechnical Engineering for Transportation Projects (GSP 126), *ASCE Proceedings of GeoTrans 2004*, 787-796.

Wells, D.L., and Coppersmith, K.J. (1994). New Empirical Relationships among Magnitude, Rupture Length, Rupture Width, Rupture Area, and Surface Displacement. *Bulletin of the Seismological Society of America*, **84**, 974-1002.

Youngs, R. and Coppersmith, K. (1985). Implications of fault slip rates and earthquake recurrence models to probabilistic seismic hazard estimates. *Bulletin of the Seismological Society of America,* **75**, 939-964.

14. ATTACHMENTS:

Attachment 1	Petersen et al. (2004)
Attachment 2	Abrahamson, Norman (2009)

EVALUATING FAULT RUPTURE HAZARD FOR STRIKE-SLIP EARTHQUAKES

Mark Petersen[1], Tianqing Cao[2], Tim Dawson[3], Arthur Frankel[4], Chris Wills[5], and David Schwartz[6]

ABSTRACT: We present fault displacement data, regressions, and a methodology to calculate in both a probabilistic and deterministic framework the fault rupture hazard for strike-slip faults. To assess this hazard we consider: (1) the size of the earthquake and probability that it will rupture to the surface, (2) the rate of all potential earthquakes on the fault (3) the distance of the site along and from the mapped fault, (4) the complexity of the fault and quality of the fault mapping, (5) the size of the structure that will be placed at the site, and (6) the potential and size of displacements along or near the fault. Probabilistic fault rupture hazard analysis should be an important consideration in design of structures or lifelines that are located within about 50m of well-mapped active faults.

INTRODUCTION

Earthquake displacements can cause significant damage to structures and lifelines located on or near the causative fault. Recent fault ruptures from earthquakes have caused failure or near-failure on bridges (Japan, 1995; Taiwan, 1999; Turkey, 1999), dams (Taiwan, 1999) and buildings (California, 1971). Earthquake ruptures in the 1971 San Fernando, California earthquake (M 6.7) caused extensive structural damage and resulted in to prevent construction of habitable buildings on the surface trace of an active fault. However, it may not be possible to relocate many structures and lifelines away from an active fault and loss of these facilities can significantly impact society. Therefore, it is essential to consider the effects of fault rupture displacements when designing structures near fault sources. The 2002 Denali earthquake showed that major

[1] U.S. Geological Survey, Golden, CO, USA. E-mail: mpetersen@usgs.gov
[2] California Geological Survey, Sacramento, CA, USA. E-mail: tcao@consrv.ca.gov
[3] U.S. Geological Survey, Menlo Park, CA, USA. E-mail: tdawson@usgs.gov
[4] U.S. Geological Survey, Golden, CO, USA. E-mail: afrankel@usgs.gov
[5] California Geological Survey, Sacramento, CA, USA. E-mail: cwills@consrv.ca.gov
[6] U.S. Geological Survey, Menlo Park, CA, USA. E-mail: schwartz@usgs.gov

lifeline structures can be designed to accommodate fault displacement if the potential for location and size of displacement is known.

The methodology presented here is an extension of the probabilistic fault displacement hazard assessments of Stepp et al. (2001) and Youngs et al. (2002) for the proposed Yucca Mountain high-level nuclear waste repository in Nevada and of Braun (2000) for the Wasatch Fault in central Utah. We present fault rupture data and a methodology to assess fault rupture hazard. The overall goal of the project is the development of improved design-oriented conditional probability models needed for estimating fault rupture hazard within either a deterministic or probabilistic framework.

METHODOLOGY

Several parameters are important in determining the fault rupture hazard at a site: (1) the size of the earthquake and probability that it will rupture to the surface, (2) the rate of all potential earthquakes on the fault (3) the distance of the site along and from the mapped fault, (4) the complexity of the fault and quality of the fault mapping, (5) the size of the structure that will be placed at the site, and (6) the potential and size of displacements along or near the fault. To develop the methodology, we consider a fault and site *(x,y)* as shown in Figure 1. The structure has a footprint with dimension *z* that is located a distance r from the fault and a distance *l*, measured from the nearest point on the fault to the end of the rupture, point *P*. The rupture in this case does not extend along the entire fault length and ruptures a section located a distance *s* from the end of the fault. The displacement on the fault has as intensity *D* and the displacement at a site off the fault has intensity *d*.

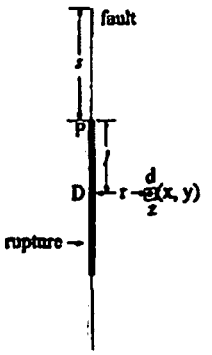

FIG. 1: Definition of variables used in the fault rupture hazard analysis

For assessing the fault rupture hazard we construct five probability density functions that describe parameters that influence the displacement on or near a fault rupture. The first two probability density functions characterize the magnitude and location of ruptures on a fault ($f_M(m)$, $f_s(s)$), the next density function characterizes the distance from the site to all potential ruptures ($f_R(r)$) and the last two probability density functions define the displacements at that site ($f_{Z,R,M}(P)$, $f_D(D(D_{max},l))$).

The first probability density function, $f_M(m)$, describes the magnitude-frequency distribution along a fault. Typically, in hazard analysis it is assumed that a fault has a preferred size of rupture, that can be determined from consideration of the physical constraints on the length or area of the fault, complexity of the fault along strike, crustal rheological properties along the fault, or rupture history. The size of the earthquake given the fault dimensions is also uncertain (Wells and Coppersmith, 1993;1994). From all known potential rupture scenarios, we develop a probability density function for the various sizes of earthquakes along the fault.

Once we determine the potential sizes of the earthquakes, we need to assess how often these ruptures occur. We define a rate parameter, α, that constrains how often the earthquakes occur in the model. This rate parameter is based on the long-term fault slip-rate, paleoseismic rate of large earthquakes, or the rate of historical earthquakes. The density function for the magnitude frequency in conjunction with the annualized rate parameter defines the frequency of each earthquake rupture along the fault.

The second probability density function describes the probability of a rupture at a specific place along a fault, $f_s(s)$. We consider the potential for the partial rupture occurring over various portions of the fault. The range of s is from zero to the fault length minus the rupture length. If the rupture is distributed uniformly along the fault, then $f_s(s)$ is a constant, which is equal to one over the fault length minus the rupture length.

If we simply consider magnitude and rupture variability, the probability that displacement d is greater than or equal to d_0 at a location (x,y) and with a foundation size z is given by:

$$\lambda(d \geq d_0)_{xyz} = \alpha \int_m f_M(m) \int_s f_s(s) P[sr \neq 0 | m] P[d \neq 0 | l,r,m,z,sr \neq 0] P[d \geq d_0 | l,r,m,d \neq 0] ds dn, \quad (1)$$

where $P[sr \neq 0/m]$ is the probability of having surface rupture given a magnitude m event. This term accounts for the possibility that an earthquake rupture on a fault will not reach the surface. For example, the 1989 Loma Prieta (M 6.9) and 1994 Northridge (M 6.7) earthquakes did not extend up to the surface and would not present a fault rupture hazard. We obtain this probability from regressions of global earthquake ruptures as published by Wells and Coppersmith (1993,1994). The term $P[d \neq 0 | l,r,m,z,sr \neq 0]$ represents the probability of having non-zero displacement at a location (l,r) for a foundation size z given magnitude m event with surface rupture, and $P[d \geq d_0 \mid l,r,m,d \neq 0]$ is the probability of the non-zero displacement d greater than or equal to a given value d_0 at a location (r,l). When the site is located on the main fault $(r=0)$ we use D to denote the displacement at $(r=0,l)$ and then (1) becomes:

$$\lambda(d \geq d_0)_{xyz} =$$

$$\alpha \int_m f_M(m) \int_s f_s(s) P[sr \neq 0 \mid m] P[D \neq 0 \mid l, r = 0, m, z, sr \neq 0] P[D \geq d_0 \mid l, r = 0, m, D \neq 0] ds dm$$

The data indicate a discontinuity between $P[d \neq 0 \mid l, r \to 0, m, z, sr \neq 0]$ and $P[D \neq 0 \mid l, r = 0, m, z, sr \neq 0]$ as well as a discontinuity between $P[D \geq d_0 \mid l, r = 0, m, D \neq 0]$ and $P[d \geq d_0 \mid l, r \to 0, m, d \neq 0]$.

The third probability density function defines the distance perpendicular to the fault. If the fault has multiple strands that could rupture in an earthquake, this aleatory variability should be considered in the fault rupture hazard model. This is not due to the fault mapping quality, which is epistemic and treated in a logic tree. We define a density function $f_R(r)$ to denote the variability, the expected rate (1) becomes:

$$\lambda(d \geq d_0)_{xyz} = \alpha \int_m f_M(m) \int_S f_s(s) P[sr \neq 0 \mid m] \int_r P[d \neq 0 \mid l, r, m, z, sr \neq 0] P[d \geq d_0 \mid l, r, m, d \neq 0] f_R(r) dr ds dl. \quad (2)$$

We need to take into account the size of the structure that will be placed at the site. We define a probability density function for the surface displacement given the structural footprint size, the distance from the fault, and the magnitude of the earthquake that ruptures the surface. The Probability $P[d \neq 0 \mid l, r, m, z, sr \neq 0]$ is not a constant for a given distance r and grid size z. It should also depend on l and m. Our data do not allow us to derive these relations for l, therefore, for this analysis we have ignored the dependences on l. From these data we can derive a density function $f_{Z,R,M}(p)$ for the above probability to have value p for a given grid size z, distance r, and magnitude.

$$\lambda(d \geq d_0)_{xyz} = \alpha \int_m f_M(m) \int_s f_S(s) P[sr \neq 0 \mid m] \int_r f_R(r) \int_p f_{Z,R,M}(p) p P[d \geq d_0 \mid l, r, m, d \neq 0] dp dr ds dm, \quad (3)$$

Finally, we develop a probability density function for displacements along the main fault $f_D(D(D_{max}, l))$. The magnitude m is related to the probability of $d \geq d_0$ through the displacement D on the main fault at a point nearest to the site (x,y) that is a function of the maximum displacement (usually at middle of the fault rupture) D_{max} and the location of this point on the rupture (l) or $D = D(D_{max}, l)$. The displacement on the fault D has aleatory variability also. Therefore, we have:

$$P[d \geq d_0 \mid l, r, m, d \neq 0] = \int_D P[d \geq d_0 \mid D(D_{max}, l), d \neq 0] f_D(D(D_{max}, l)) dD \quad (4)$$

where $f_D(D(D_{max}, l))$ is the density function for $D = D(D_{max}, l)$ given magnitude m and location l. If formula (4) is inserted into (3), we get the final formula with aleatory variability of rupture distribution on the fault, multiple fault rupture traces, displacement variability on the main fault, and probability variability of having non-zero displacement. The final formula for the probabilistic fault rupture hazard is:

$$\lambda(d \geq d_0)_{xyz} = \alpha \int_m f_M(m) \int_s f_S(s) P[sr \neq 0 \mid m] \int_r f_R(r) \int_p f_{Z,R,M}(p) p \times$$

$$\int_D f_D(D(D_{max}, l)) P[d \geq d_0 \mid D(D_{max}, l), d \neq 0] dD dp dr ds dm \quad (5)$$

This formula is used to assess the probabilistic fault rupture hazard at a site. If one desires to calculate the deterministic fault rupture hazard the formula would be

modified by eliminating the rate parameter, α, from the equation. Alternatively, one could calculate the median displacement for a particular earthquake using the empirical data and relations that are described below.

DATA AND REGRESSIONS

Following earthquakes that rupture the ground surface, geologists have prepared detailed maps and measured displacement along the surface trace. We collected displacement data from published measurements obtained from studies of several large strike-slip earthquakes: 1968 Borrego Mountain (M6.6), 1979 Imperial Valley (M6.5), 1987 Elmore Ranch (M6.2), 1987 Superstition Hills (M 6.6), 1995 Kobe (M6.9), 1992 Landers (M7.3), 1999 Izmit (M7.4), and the 1999 Hector Mine (M7.1) (Figure 2).

This fault displacement data is used with earthquake recurrence information provided by the National Seismic Hazard maps (Petersen et al., 1996; Frankel et al., 2002). To evaluate the fault hazard at a site we need to answer three questions: 1).Where will future fault displacements occur? 2).How often do surface displacements occur? 3). How much displacement can occur at the site? In this section we will discuss the data and model regressions that are used to evaluate each of these questions in a probabilistic sense.

Where will future fault displacements occur?

The primary method of assessing where future ruptures will occur is to identify sites of past earthquakes. We can identify these potential rupture sources by studying historic earthquake ruptures, defining seismicity patterns, and identifying active faults.

Historical ruptures are an important dataset to interpret future fault ruptures. Figure 2 shows examples of historic strike-slip earthquake rupture traces that have been used in this hazard assessment. These traces show a wide variety of rupture patterns. The largest fault displacements are along the principal fault, but significant displacements may also occur on distributed ruptures located several meters to kilometers away from the main fault. The displacement values are not shown, but have been compiled in ARC GIS files. The rupture patterns for a single earthquake may be fairly simple in some regions but quite complex in others, characterized by discontinuous faulting that occurs over a broad zone.

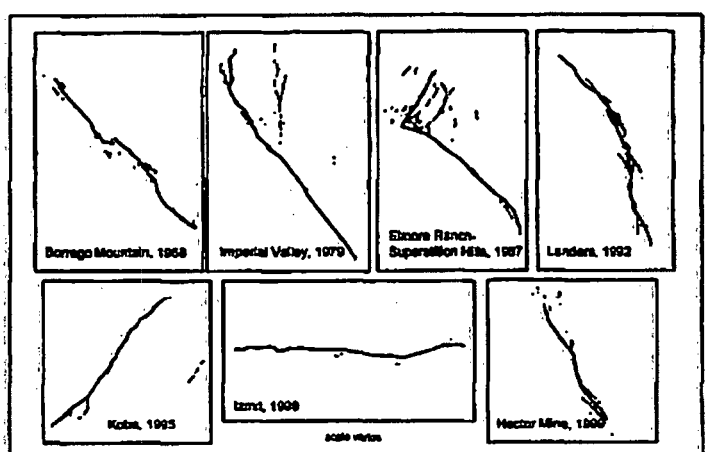

FIG. 2: Traces of faults used in analysis

Active faults are places where the likelihood is greatest that we will have future earthquakes. In California, legislation requires that the State

Geologist identify those faults that are "sufficiently active and well-defined" to represent a surface rupture hazard. In order to do this, the California Geological Survey has examined the majority of the potentially active faults in the state and prepared detailed maps of those that can be shown to have ruptured to the ground surface in Holocene time. These faults are included in "Alquist-Priolo Earthquake Fault Zones" (A-P zones), which regulate development near active fault traces. In our analysis we have compared the maps of faults within A-P zones prepared before surface-rupturing earthquakes with maps of the actual surface rupture mapped following the event. This type of analysis provides a measure of the uncertainty in accurately locating future ruptures.

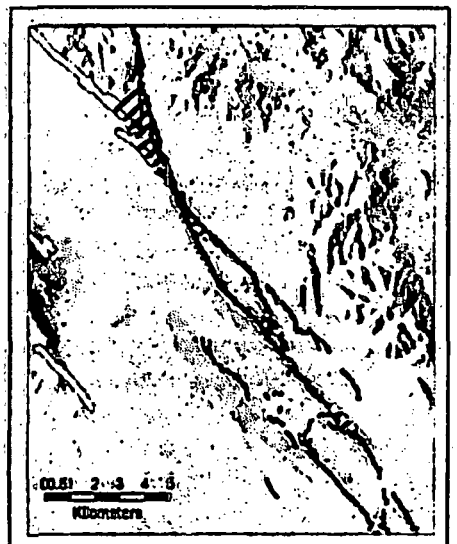

FIG 3: Comparison of previously mapped A-P fault (white) and 1999 Hector Mine earthquake surface rupture (black)

The 1999 Hector Mine earthquake is an example of an event that ruptured along a fault that had been mapped prior to the earthquake rupture. CGS had evaluated the Bullion fault and established A-P zones in 1988 (Hart, 1987). The 1999 event ruptured part of the Bullion fault (Figure 3). Much of the rupture occurred close to the previously mapped fault. Much of the northern part of the rupture occurred on a fault east of the Bullion fault that had been previously mapped, but not evaluated for A-P zones because it lies in such a remote area. The event also ruptured secondary faults over a wide area at the south end of the rupture. In evaluating the potential for surface fault displacements, we need to account for the potential that significant displacement can occur on previously unmapped faults and that secondary displacement can occur over a broad area.

The accuracy of mapping and complexity of the fault trace parameters are handled in a logic tree to account for our uncertainty in estimating the location of the fault traces. Faults mapped for A-P zones show the surface traces of the faults in four categories based on how clearly and precisely they can be located. We compared the fault traces mapped in each of these categories with later surface rupture. In general, the regressions show faults where a geologist is more confident of the location more accurately predict the surface rupture location, although these distinctions are not as clear as one might expect. We also examined the A-P fault traces and characterized them as "simple" or "complex". We expect that surface rupture will be more distributed and not as accurately predicted at "complex" fault bends, stopovers, branch points, and ends than on "simple" straight traces. The regressions comparing the A-P fault traces with the later surface rupture will allow us to determine if and how much the fault complexity influences our ability to predict the location of fault rupture.

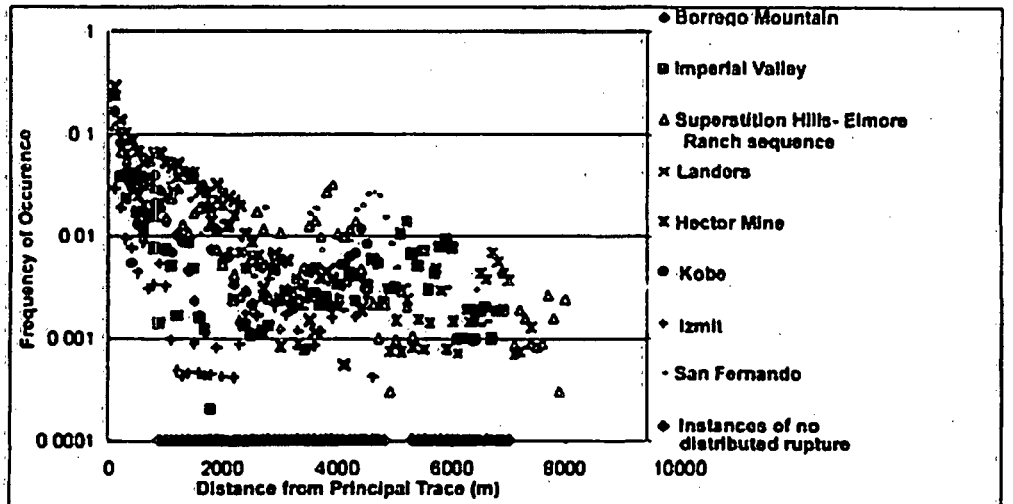

FIG 4: Frequency of earthquake displacements within 50 m cells as a function distance from principal trace

How often do surface displacements occur?

To answer the question of how often surface fault displacements occur, requires assessing the magnitudes of earthquakes that may rupture a fault, the rate of occurrence of these earthquakes, the potential for ruptures on a fault to pass by the site, and the potential for the modeled earthquakes to rupture the surface. CGS amd USGS have developed earthquake source models for earthquake ground shaking hazard assessment (Petersen et al.(1996); Frankel et al. (2002). These models identify earthquake magnitudes, rates, and ruptures that can be used in a fault displacement hazard analysis for the United States. We calculate the number of ruptures that will pass by the site by considering the total fault length and the rupture length for each magnitude. Assessing the rates of occurrence of earthquakes is pertinent to probabilistic fault displacement hazard analysis but not necessary for the deterministic analysis. A deterministic analysis simply gives a median (or some other fractile) displacement assuming that the event occurs.

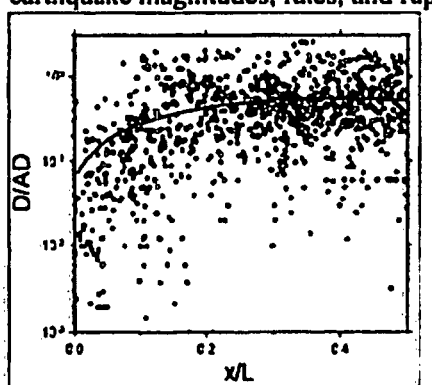

FIG 5: Displacement data on the fault. The y-axis indicates the measured displacement divided by the average displacement and the x-axis indicates the distance from the end of the fault x divided by the total length of the rupture.

How much displacement can occur at the site?

To assess probabilistic displacement hazard at a site, it is necessary to understand the potential for rupture at that site and the distribution of displacements. The probability of experiencing displacements on a fault, given that a large earthquake occurs, is typically greater than 50%

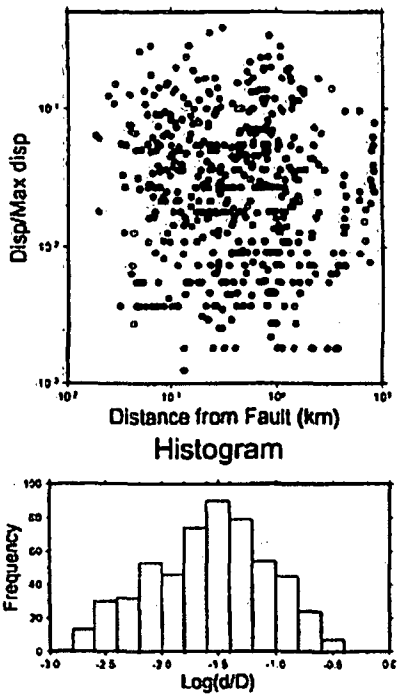

FIG 6: Displacement data for sites located off the fault. (A) A plot of normalized displacements (displacement divided by the maximum displacement on the fault) as a function of distance (with Superstition Hills data removed) and (B) a histogram showing the frequency of $\log_{10}$ normalized displacements for all the data shown in A.

and the displacements can be measured in meters. In contrast, the probability of experiencing displacements at a site located a few hundred meters away is typically much lower (usually less than 30%) and the displacements will probably be measured in centimeters rather than meters. Most of the 50 m cells located away from the fault do not experience distributed displacements unless there is complexity in the fault trace.

Following the method of Youngs at al (2002) we analyzed the potential for distributed fault displacement to pass through an area as a function of distance from the principal trace. We performed regressions on the displacement data to analyze the rupture potential in different footprint areas. Figure 4 shows the frequency of occurrence of a rupture in a 50 m footprint for each of the different earthquakes.

The footprint size is critical in calculating the probability of rupture at a site. Typically the smaller footprints have lower probability of containing a rupture. The frequency is very high for distances very close to the fault. However, this frequency drops off quickly and there is only about a 1 in 100 chance of having rupture within a 50 m footprint if the distance is more than about 2 kilometers. The displacement data indicate that most of the displacements occur on or within a few hundred meters of the principal fault.

Once we have calculated the likelihood for having displacements pass through a given area, we need to define a distribution of the displacements. We separate the data into on-fault and off-fault displacements. Figure 5 shows the displacements along the strike of the fault. We performed a polynomial regression on the on-fault data to obtain the typical distribution of displacements along a fault. In general the displacements are largest near the middle of the fault and falls off rapidly within about 10% of the end of the rupture. The displacement data indicate that most of the displacements occur on or within a few hundred meters of the principal fault. Figure 6 shows of the normalized off-fault displacements as a function of distance. The data indicates almost no correlation of displacements with distance. Displacements are typically quite small. The histogram indicates that the mode of the data is centered at about $10^{(-1.5)} = 0.03$, or

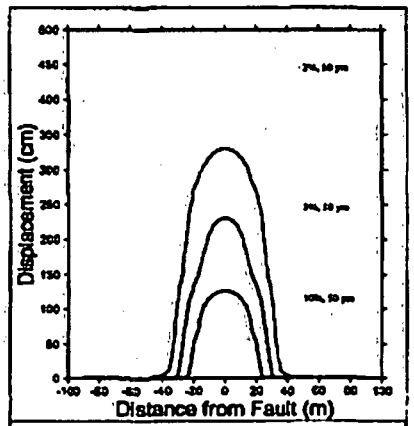

Figure 8: Example of fault displacement hazard on a transect that crosses the fault.

about 3% of the displacements observed on the principal fault. Displacements range from less than 1% to about 32% of the values observed on the fault.

DISCUSSION

We have assembled data on world-wide strike-slip earthquake surface rupture and compared it with pre-rupture fault mapping. In California, the fault maps prepared for the Alquist-Priolo Earthquake Fault Zones Act provide a uniform, detailed set of pre-rupture fault maps that are the basis for comparison for most of our data. We have analyzed the distribution of fault displacement about previously mapped fault traces and used that analysis to construct a system for evaluating the hazard of fault displacement.

In order to consider the probability for surface fault displacement at a site, one must consider the rates of earthquakes on significant active nearby faults. For California, most of the activity rates for faults have been compiled and used in the National Seismic Hazard Maps. For earthquakes that rupture to the ground surface, we can obtain probabilistic estimates of displacement from the regressions for this study.

We developed regressions for fault displacement considering that most earthquakes do not rupture entire faults, that the fault displacement tends to die-out rapidly near the ends of a rupture and that fault rupture does not always follow previously mapped faults. Maps of faults prepared before the rupture show faults with varying levels of perceived accuracy. Our regressions show that more accurately mapped faults correlate better with subsequent fault rupture, but the differences are not great. Surface displacements also tend to show greater complexity in areas where the fault geometry is complicated. Later regressions will include the potential for more broadly distributed displacement at fault bends, stopovers, branches and ends.

To illustrate the methodology and datasets, we assume a fault that has which has a characteristic magnitude 7.26 and with a recurrence of 167 years. This recurrence leads to an annual rate of 0.006 earthquakes per year. Figure 7 shows the calculated displacement hazard on a line perpendicular to the fault. For this illustration, the fault trace location is assumed to be well located, with a standard deviation of 10 meters. The amplitude of the displacement hazards is controlled by the characteristic magnitude, recurrence rate, and the duration of the exposure for the hazards.

Using the formulation and data developed in this study, one can estimate the potential for surface fault displacement within an area of a lifeline or other project. The input required for this analysis includes the rate of earthquakes of various

magnitudes on a nearby fault or faults; the distance from the active fault; the accuracy of the nearest fault trace on the detailed map; and the size of the site to be considered. Output of the analysis is the amount of displacement with a specified probability or corresponding to a particular deterministic earthquake. The potential displacement considers the potential displacement along the fault, the potential that the location of the fault varies from where it was mapped and the potential for distributed displacement around the trace of the fault.

ACKNOWLEDGEMENTS

We would like to especially thank the Pacific Earthquake Engineering Research Center (PEER Lifelines project# 1J02,1J02,1J03) advisory groups that assisted us in the formulation and implementation of these results. These members include: Norm Abrahamson, Lloyd Cluff, Brian Chiou, Cliff Roblee, Bill Bryant, Jon Bray, Tom Rockwell, Donald Wells, Bob Youngs, and Clarence Allen.

REFERENCES

Braun, J.B. 2000 "Probabilistic fault displacement hazards of the Wasatch fault, Utah." Dept. of Geology and Geophysics, The University of Utah (Masters thesis).

Frankel, A.D., Petersen, M.D., Mueller, C.S., Haller, K.M., Wheeler, R.L., Leyendecker, E.V., Wesson, R.L., Harmsen, S.C., Cramer, C.H., and Perkins, D.M. (2002) "Documentation for the 2002 update of the National Seismic Hazard Map" U.S. G. S. Open-file Report 02-420.

Hart, E.W., 1987, "Pisgah, Bullion and related faults" California Division of Mines and Geology Fault Evaluation Report FER-188, 14 p.

Petersen, M.D., Bryant, W.A., Cramer, C.H., Cao, T., Reichle, M.S., Frankel, A.D., Lienkaemper, J.J., McCrory, P.A., and Schwartz, D.P. (1996) "Probabilistic seismic hazard assessment for the state of California." California Div. of Mines and Geology Open-file Report 96-08 and U.S. G. S. Open-file Report 96-706.

Stepp, J.C., Wong, I., Whitney, J., Quittmeyer, R., Abrahamson, N., Toro, G., Youngs, R., Coppersmith, K., Savy, J., Sullivan, T., and Yucca Mountain PSHA Project Members. 2001 "Probabilistic seismic hazard analyses for ground motions and fault displacement at Yucca Mountain, Nevada." *Earthquake Spectra*; 17(1): 113-150.

Wells, D.L. and Coppersmith, K.J. 1993 "Likelihood of surface rupture as a function of magnitude (abs.)." *Seismological Research Letters*; 64(1): p54.

Wells, D.L and Coppersmith, K.J. 1994 "New empirical relationships among magnitude, rupture length, rupture width, rupture area, and surface displacement." *Bulletin of the Seismological Society of America*; 84: 974-1002.

Youngs, R.R., Arabasz, W.J., Anderson, R.E., Ramelli, A.R., Ake, J.P., Slemmons, D.B., McCalpin, J.P., Doser, D.I., Fridrich, C.J., Swan, F.H. III, Rogers, A.M., Yount, J.C., Anderson, L.W., Smith, K.D., Bruhn, R.L., Knuepfer, L.K., Smith, R.B., dePolo, C.M., O'Leary, K.W., Coppersmith, K.J., Pezzopane, S.K., Schwartz, D.P., Whitney, J.W., Olig, S.S., and Toro, G.R. 2002 "A methodology for probabilistic fault displacement hazard analysis (PFDHA)." *Earthquake Spectra*;

UC Berkeley seismic hazard lecture notes by Dr. Norm Abrahamson, 2009

6 Source Characterization

Source characterization describes the rate at which earthquakes of a given magnitude, and dimensions (length and width) occur at a given location. For each seismic source, the source characterization develops a suite of credible and relevant earthquake scenarios (magnitude, dimension, and location) and computes the rate at which each earthquake scenario occurs.

The first step in the source characterization is to develop a model of the geometry of the sources. There are two basic approaches used to model geometries of seismic sources in hazard analyses: areal source zone and faults sources.

Once the source geometry has been modelled, then models are then developed to describe the occurrence of earthquakes on the source. This includes models that describe the distribution of earthquake magnitudes, the distribution of rupture dimensions for each earthquake magnitude, the distribution of locations of the earthquakes for each rupture dimension, and the rate at which earthquakes occur on the source (above some minimum magnitude of interest).

6.1 Geometrical Models Used for Seismic Sources in Hazard Analyses

In the 1970s and early 1980s, the seismic source characterization was typically based on historical seismicity data using seismic zones (called areal sources). In many parts of the world, particularly those without known faults, this is still the standard of practice. In regions with geologic information on the faults (slip-rates or recurrence intervals), the geologic information can be used to define the activity rates of faults.

6.1.1. Areal Source Zones

Areal source zones are used to model the spatial distribution of seismicity in regions with unknown fault locations. In general, the areal source zone is a volume; there is a range on the depths of the seismicity in addition to the plot of the zone in map view.

Even for regions with known faults, background zones modeled as areal sources are commonly included in the source characterization to account for earthquakes that occur off of the known faults.

Gridded seismicity is another type of areal source. In this model the dimensions of the areal source zones are small. The seismicity rate for each small zone is not based solely on the historical seismicity that has occurred in the small zone, but rather it is based on the smoothed seismicity smoothed over a much larger region. This method of smoothed seismicity has been used by the USGS in the development of national hazard maps (e.g. Frankel et al, 1996).

6.1.2 Fault Sources

Fault sources were initially modelled as multi-linear line sources. Now they are more commonly modelled as multi-planar features. The earthquake ruptures are distributed over the fault plane. Usually, the rupture are uniformly distributed along the fault strike, but may have a non-uniform distribution along strike.

6.2 Seismic moment, moment magnitude, and stress-drop

We begin with some important equations in seismology that provide a theoretical basis for the source scaling relations. The seismic moment, M_o (in dyne-cm), of an earthquake is given by

$$M_o = \mu A D \qquad (6.1)$$

where μ is the shear modulus of the crust (in dyne/cm^2), A is the area of the fault rupture (in cm^2), and D is the average displacement (slip) over the rupture surface (in cm). For the crust, a typical value of μ is 3×10^{11} dyne/cm^2.

The moment magnitude, M, defined by Hanks and Kanamori (1979) is

$$M = \frac{2}{3}\log_{10}(M_o) - 10.7 \qquad (6.2)$$

The relation for seismic moment as a function of magnitude is

$$\log_{10} M_o = 1.5\,M + 16.05 \qquad (6.3)$$

Note that since eq. (6.2) is a definition, the constant, 16.05, in eq. (6.3) should not be rounded to 16.1.

These equations are important because they allow us to relate the magnitude of the earthquake to physical properties of the earthquake. Substituting the eq.(6.2) into eq. (6.1) shows that the magnitude is related to the rupture area and average slip.

$$M_w = \frac{2}{3}\log(A) + \frac{2}{3}\log(D) + \frac{2}{3}\log(\mu) - 10.7 \qquad (6.4)$$

The rupture area, A, and the average rupture displacement, D, are related through the stress-drop. In general terms, the stress-drop of an earthquake describes the compactness of the seismic moment release in space and/or time. A high stress-drop indicates that the moment release is tightly compacted in space and/or time. A low stress-drop indicates that the moment release is spread out in space and/or time. There are several different measures of stress-drop used in seismology. Typically, they are all just called "stress-drop". In this section, we will refer to the static stress-drop which is a measure of the compactness of the source in space only.

For a circular rupture, the static stress-drop at the center of the rupture is given by

$$\Delta\sigma_{circ} = \frac{7x10^{-6}}{16}\pi^{1.5}\,\mu\frac{D}{\sqrt{A}} \qquad (6.5)$$

where $\Delta\sigma$ is on bars (Kanamori and Anderson, 1979). The constants will change for other rupture geometries (e.g. rectangular faults) and depending on the how the stress-drop is defined (e.g. stress-drop at the center of the rupture, or average stress-drop over the rupture plane).

A circular rupture is reasonable for small and moderate magnitude earthquakes (e.g. M<6), but for large earthquakes a rectangular shape is more appropriate. For a finite rectangular fault, Sato (1972) showed that the stress-drop is dependent on the aspect ratio (Length / Width). Based on the results of Sato, the stress-drop for a rectangular fault scales approximately as $(L/W)^{-0.15}$. Using this scaling and assuming that L=W for a circular crack, eq. (6.5) can be generalized as

$$\Delta\sigma_{rec} = \frac{7x10^{-6}}{16}\pi^{1.5}\mu\frac{D}{\sqrt{A}}\left(\frac{L}{W}\right)^{-0.15} \qquad (6.6)$$

Note that eq. (6.6) is not directly from Sata (1972), since he computed the average stress-drop over the fault. Here, I have used constants such that rectangular fault with an aspect ratio of 1.0 is equal to the stress-drop for a circular crack. The absolute numerical value of the stress-drop is not critical for our purposes here. The key is that the stress-drop is proportional to D/sqrt(A) with a weak dependence on the aspect ratio. For an aspect ratio of 10, the stress-drop given by eq. (6.6) is 30% smaller than for a circular crack (eq. 6.5).

If the median value of D/sqrt(A) does not depend on earthquake magnitude and the dependence on the aspect ratio is ignored, then the stress-drop will independent of magnitude which simplifies the source scaling relation given in eq. (6.4). Let

$$c_1 = \frac{D}{\sqrt{A}} \qquad (6.7)$$

and assuming $\mu = 3 \times 10^{11}$ dyne/cm^2, then eq (6-4) becomes

$$\overline{M} = \log(A) + \frac{2}{3}\log(c_1) - 3.05 \qquad (6.8)$$

where $\overline{M}$ is the mean magnitude for a given rupture area.

For a constant median static stress-drop, magnitude is a linear function of the log(A) with a slope of 1.0. That is,

$$M = \log(A) + b \tag{6.9}$$

where b is a constant that depends on the median stress-drop. For individual earthquakes, there will be aleatory variability about the mean magnitude.

It has been suggested that the static stress-drop may be dependent on the slip-rate of the fault (Kanamori 1979). In this model, faults with low slip-rates have higher static stress-drops (e.g. smaller rupture area for the given magnitude) than faults with high slip-rates. This implies that the constant, b, in eq. (6-9) will be dependent on slip-rate.

6.2.1 Other magnitude scales

While moment magnitude is the preferred magnitude scale, the moment magnitude is not available for many historical earthquakes. Other magnitude scales that are commonly available are body wave magnitude (m_b), surface wave magnitude (M_S), and local magnitude (M_L). The m_b and M_L magnitudes typically are from periods of about 1 second and the M_S is from a period of about 20 seconds. These different magnitude scales all give about the same value in the magnitude 5 to 6 range (Figure 6-1). As the moment magnitude increases, the difference between the magniude scales increases. This is caused because the short period magnitude measures (m_b and M_L) saturate at about magnitude 7 and the long period magnitude measures (M_S) begin to saturate at about magnitude 8.0.

There are various conversion equations that have been developed to convert the magnitudes of older earthquakes to moment magnitude. Figure 6-1 shows and example of these conversions. When developing an earthquake catalog for a PSHA, it is important to take these conversions into account.

6.3 "Maximum" Magnitude

Once the source geometry is defined, the next step in the source characterization is to estimate the magnitude of largest earthquakes that could occur on a source.

For areal sources, the estimation of the maximum magnitude has traditionally been computed by considering the largest historical earthquake in the source zone and adding some additional value (e.g. half magnitude unit). For source zones with low historical seismicity rates, such as the Eastern United States, then the largest historical earthquake from regions with similar tectonic regimes are also used.

For fault sources, the maximum magnitude is usually computed based on the fault dimensions (length or area). Prior to the 1980s, it was common to estimate the maximum magnitude of faults assuming that the largest earthquake will rupture 1/4 to 1/2 of the total fault length. In modern studies, fault segmentation is often used to constrain the rupture dimensions. Using the fault segmentation approach, geometric discontinuities in the fault are sometimes identified as features that may stop ruptures. An example of a discontinuity would be a "step-over" in which the fault trace has a discontinuity. Fault step-overs of several km or more are often considered to be segmentation points. The segmentation point define the maximum dimension of the rupture, which in tern defines the characteristic magnitude for the segment. The magnitude of the rupture of a segment is called the "characteristic magnitude".

The concept of fault segmenation has been called into question following the 1992 Landers earthquake which ruptured multiple segments, including rupturing through several apparent segmentation points. As a result of this event, multi-segment ruptures are also considered in defining the characteristic earthquakes,

Before going on with this section, we need to deal with a terminology problem. The term "maxmimum" magnitude is commonly used in seismic hazard analyses, but in many cases it is not a true maximum. The source scaling relations that are discussed below are empirically based models of the form shown in eq. 6.9). If the entire fault area ruptures, then the magnitude given by eq. (6.9) is the mean magnitude for full fault rupture. There is still significant aleatory variability about this mean magnitude.

For example, the using an aleatory variability of 0.25 magnitude units, the distribution of magnitudes for a mean magnitude of 7.0 is shown in Figure 6-2. The mean magnitude (point A) is computed from a magnitude area relation of the form of eq.

(6.9). The true maximum magnitude is the magnitude at which the magnitude distribution is truncated. In Figure 6-2, the maximum magnitude shown as point B is based on 2 standard deviations above the mean. In practice, it is common to see the mean magnitude listed as the "maximum magnitude". Some of the ideas for less confusing notation are awkward. For example, the term "mean maximum magnitude" could be used, but this is already used for describing the average "maximum magnitude" from alternative scaling relations (e.g. through logic trees). In this report, the term "mean characteristic magnitude" will be used for the mean magnitude for full rupture of a fault.

The mean characteristic magnitude is estimated using source scaling relations based on either the fault area or the fault length. These two approaches are discussed below.

6.3.1 Magnitude-Area Relations

Evaluations of empirical data have found that the constant stress-drop scaling (as in eq. 6.9) is consistent with observations. For example, the Wells and Coppersmith (1994) magnitude-area relation for all fault types is

$$M = 0.98\,Log(A) + 4.07 \qquad (6.10)$$

with a standard deviation of 0.24 magnitude units. The estimated slope of 0.98 has a standard error of 0.04, indicating that the slope is not significantly different from 1.0. That is, the empirical data are consistent with a constant stress-drop model. The standard deviation of 0.24 magnitude units is the aleatory variability of the magnitude for a given rupture area. Part of this standard deviation may be due to measurement error in the magnitude or rupture area.

For large crustal earthquakes, the rupure reaches a maximum width due to the thickness of the crust. Once the maximum fault with is reached, the scaling relation may deviate from a simple 1.0 slope. In particular, how does the average fault slip, D, scale once the maximum width is reached? Two models commonly used in seismiology are the W-model and the L-model. In the W-model, D scales only with the rupture width and does not increase once the full rupture width is reached. In the

L-model, D is proportional to the rupture length. A third model is a constant stress-drop model in which the stress-drop remains constant even after the full fault width is reached.

Past studies have shown that for large earthquake that were depth limited (e.g. the rupture went through the full crustal thickness), the average displacement average continues to increase as a function of the fault length, indicating that the W-model is not appropriate. Using an L-model ($D = \alpha L$), then $A=L\ W_{max}$ and eq. (6.4) becomes

$$M = \frac{4}{3}\log(L) + \frac{2}{3}\log(W_{max}) + \frac{2}{3}\log(\alpha) + \frac{2}{3}\log(\mu) - 10.7 \qquad (6.11)$$

Combining all of the constants together leads to

$$M = \frac{4}{3}\log(L) + b_1 = \frac{4}{3}\log(A) + b_2 \qquad (6.12)$$

So for an L-model, once the full fault width is reached, the slope on the log(L) or log(A) term is 4/3. Hanks and Bakun (2001) developed a magnitude-area model that incorporates an L-model for strike-slip earthquakes in California (Table 6-1). In their model, the transition from a constant stress-drop model to an L-model occurs for a rupture area of 468 km^2 (Figure 6-3). For and aspect ratio of 2, this transition area corresponds to a fault width of 15 km.

Table 6-1. Examples of magnitude-area scaling relations for crustal faults

	Mean Magnitude	Standard Deviation
Wells and Coppersmith (1994) all fault types	M = 0.98 Log (A) + 4.07	σ_m=0.24
Wells and Coppersmith (1994) strike-slip	M = 1.02 Log(A) + 3.98	σ_m=0.23
Wells and Coppersmith (1994) reverse	M = 0.90 Log(A) + 4.33	σ_m=0.25
Ellsworth (2001) strike-slip for A> 500 km^2	M = log(A) + 4.1 (lower range: 2.5th percentile) M = log(A) + 4.2 (best estimate) M = log(A) + 4.3 (upper range: 97.5th percentile)	σ_m=0.12
Hanks and Bakun	M = log(A) + 3.98 for A< 468 km^2	σ_m=0.12

(2001) strike-slip	M = 4/3 Log(A) + 3.09 for A> 468 km^2)	
Somerville et al (1999)	M = log(A) + 3.95	

Examining the various models listed in Table 6-1. The mean magnitude as a function of the rupture area is close to

$$M = \log(A) + 4 \qquad (6.13)$$

This simplified relation will be used in some of the examples in later sections to keep the examples simple. Its use is not meant to imply that the more precise models (such as those in Table 6-1) should not be used in practice.

Regional variations in the average stress-drop of earthquakes can be accommodated by different a constant in the scaling relation.

6.3.2 Magnitude-Length Relations

The magnitude is also commonly estimated using fault length, L, rather than rupture area. One reason given for using the rupture length rather than the rupture area is that the down-dip width of the fault is not known. The seismic moment is related to the rupture area (eq. 6.1) and using empirical models of rupture length does not provide the missing information on the fault width. Rather, it simply assumes that the average fault width of the earthquakes in the empirical database used to develop the magnitude-length relation is appropriate for the site under study. Typically, this assumption is not reviewed. A better approach is to use rupture area relations and include epistemic uncertainty in the down-dip width of the fault. This forces the uncertainty in the down-dip width to be considered and acknowledged rather than hiding it in unstated assumptions about the down-dip width implicit in the use of magnitude-length relations.

If the length–magnitude relations are developed based only on data from the region under study, and the faults have similar dips, then length-magnitude relations may be used.

6.4 Rupture Dimension Scaling Relations

The magnitude-area and magnitude-length relations described above in section 6.3 are used to compute the mean characteristic magnitude for a given fault dimension. The mean characteristic magnitude is used to define the magnitude pdf. In the hazard calculation, the scaling relations are also used to define the rupture dimensions of the scenario earthquakes. To estimate the mean characteristic magnitude, we used equations that gave the magnitude as a function of the rupture dimension (e.g. M(A)). Here, we need to have equations that gives the rupture dimensions as a function of magnitude (e.g. A(M)).

Typically, the rupture is assumed to be rectangular. Therefore, to describe the rupture dimension requires the rupture length and the rupture width. For a given magnitude, there will be aleatory variability in the rupture length and rupture width.

6.4.1 Area-Magnitude Relations

The common practice is to use empirical relations for the A(M) model; however, the empirical models based on regression are not the same for a regression of magnitude given and area versus a regression of area given magnitude. In most hazard evaluations, different models are used for estimating M(A) versus A(M). As an example, the difference between the M(A) and A(M) based on the Wells and Coppersmith (1994) model for all ruptures simply due to the regression is shown in Figure 6-4, with A on the x-axis for most models. The two models are similar, but they differ at larger magnitudes. While the application of these different models is consistent with the statistical derivation of the models, there is a problem of inconsistency when both models are used in the hazard analysis. The median rupture area for the mean characteristic earthquake computed using the A(M) model will not, in general, be the same as the fault area.

As an alternative, if the empirical models are derived with constraints on the slopes (based on constant stress-drop, for example) then the M(A) and A(M) models will be consistent. That is, applying constraints to the slopes leads to models that can be applied in either direction. As noted above, the empirically derived slopes are close to unity, implying that a constant stress-drop constraint is consistent with the observations.

6.4.2 Width-Magnitude Relations

It is common in practice to use empirical models of the rupture width as a function of magnitude. For shallow crustal earthquakes, the available fault width is limited due to the seismogenic thickness of the crust. The maximum rupture width is given by

$$W_{\max} = \frac{H_{seimo}}{\sin(dip)} \tag{6.14}$$

where H_{seismo} is the seismogenic thickness of the crustal (measured in the vertical direction). This maximum width will vary based on the crustal thickness and the fault dip. The empirical rupture width models are truncated on fault-specific basis to reflect individual fault widths. For example, if the seismogenic crust has a thickness of 15 km and a fault has a dip of 45 degrees, then the maximum width is 21 km; however, if another fault in this same region has a dip of 90 degrees, then the maximum width is 15 km.

For moderate magnitudes (e.g. M5-6), the median width from the empirical model is consistent with the width based on an aspect ratio of 1.0. At larger magnitudes, the empirical model produces much smaller rupture widths, reflecting the limits on the rupture width for the faults in the empirical data base.

Rather than using a width-magnitude model in which the slope is estimated from a regression analysis, a fault-specific width limited model can be used in which the median aspect ratio is assumed to be unity until the maximum width is reached. Using this model, the median rupture width is given by

$$\log(\overline{W}(M)) = \begin{cases} 0.5\log(A(M)) & for\ \sqrt{A(M)} < W_{\max} \\ \log(W_{\max}) & for\ \sqrt{A(M)} \geq W_{\max} \end{cases} \tag{6.15}$$

The aleatory variability of the log(W(M)) should be based on the empirical regressions for the moderate magnitude (M5.0 – 6.5) earthquakes because the widths from the larger magnitudes will tend to have less variability due to the width limitation

In the application of this model, the rupture width pdf is not simply a truncated normal distribution, but rather the area of the pdf for rupture widths greater than

W_{max} is put at W_{max}. Formally, the log rupture width model is a composite of a truncated normal distribution and a delta function. The weight given to the delta function part of the model is given by the area of the normal distribution that is above W_{max}. In practice, this composite distribution is implemented by simply setting $W=W_{max}$ for any widths greater than W_{max} predicted from the log-normal distribution.

6.5 Magnitude Distributions

In general, a seismic source will generate a range of earthquake magnitudes. That is, there is aleatory variability in the magnitude of earthquakes on a given source. If you were told that an earthquake with magnitude greater than 5.0 occurred on a fault, and then you were asked to give the magnitude, your answer would not be a single value, but rather it would be a pdf.

The magnitude pdf (often called the magnitude distribution) will be denoted $f_m(m)$. It describes the relative number of large magnitude, moderate, and small magnitude earthquakes that occur on the seismic source.

There are two general categories of magnitude density functions that are typically considered in seismic hazard analyses: the truncated exponential model and the characteristic model. These are described in detail below.

6.5.1 Truncated Exponential Model

The truncated exponential model is based on the well known Gutenberg-Richter magnitude recurrence relation. The Gutenberg-Richter relation is given by

$$Log\, N(M) = a - bM \tag{6.16}$$

where N(M) is the cumulative number of earthquakes with magnitude greater than M. The a-value is the log of the rate of earthquakes above magnitude 0 and the b-value is the slope on a semi-log plot (Figure 6-5). Since N(M) is the cumulative rate, then the derivative of N(M) is the rate per unit magnitude. This derivative is proportional to the magnitude pdf.

The density function for the truncated exponential model is given in Section 4. If the model is truncated a M_{min} and M_{max}, then the magnitude pdf is given by

$$f_m^{TE}(m)=\frac{\beta\exp(-\beta(m-M_{min})}{1-\exp(-\beta(M_{max}-M_{min}))} \qquad (6.17)$$

where β is ln(10) times the b-value. Empirical estimates of the b-value are usually used with this model. An example of the truncated exponential distribution is shown in Figure 6-5.

6.5.2 Characteristic Earthquake Models

The exponential distribution of earthquake magnitudes works well for large regions; however, in most cases is does not work well for fault sources (Youngs and Coppersmith, (1985). As an example, Figure 6-6 shows the recurrence of small earthquakes on the south central segment of the San Andreas fault. While the small earthquakes approximate an exponential distribution, the rate of large earthquakes found using geologic studies of the recurrence of large magnitude earthquakes is nuch higher than the extrapolated exponential model. This discrepancy lead to the development of the characteristic earthquake model.

Individual faults tend to generate earthquakes of a preferred magnitude due to the geometry of the fault. The basic idea is that once a fault begins to rupture in a large earthquake, it will tend to rupture the entire fault segment. As a result, there is a "characteristic" size of earthquake that the fault tends to generate based on the dimension of the fault segment.

The fully characteristic model assumes that all of the seismic energy is released in characteristic earthquakes. This is also called the "maximum magnitude" model because it does not allow for moderate magnitude on the faults. The simplest form of this model uses a single magnitude for the characteristic earthquake (e.g. a delta function).

A more general form of the fully characteristic model is a truncated normal distribution (see Section 4) that allows a range of magnitudes for the characteristic earthquake consistent with the aleatory variability in the magnitude-area or magnitude-length relation. The distribution may be truncated at $nsig_{max}$ standard deviations above the mean characteristic magnitude. The magnitude density function for the truncated normal (TN) model is given by:

$$f_m^{TN}(M)=\begin{cases} \dfrac{1}{\sqrt{2\pi}\sigma_m}\dfrac{1}{\Phi(nsig_{\max})}\exp\left(\dfrac{-(M-\overline{M}_{char})^2}{2\sigma_m^2}\right) & for \left|\dfrac{M-\overline{M}_{char}}{\sigma_m}\right| < nsig_{\max} \\ 0 & otherwise \end{cases} \quad (6.18)$$

and M_{char} is the mean magnitude of the characteristic earthquake. An example of this model is also shown in Figure 6-5.

6.5.3 Composite Models

The fully characteristic earthquake model does not incorporate moderate magnitude earthquakes on the faults. This model is appropriate in many cases. Alternative models are based on a combination of the truncated exponential model and the characteristic model. These composite models include a characteristic earthquake distribution for the large magnitude earthquakes and an exponential distribution for the smaller magnitude earthquakes. Although they contain an exponential tail, these models are usually called characteristic models

One such composite model is the Youngs and Coppersmith (1985) characteristic model. The magnitude density function for this model is shown in Figure 6-5. This model has a uniform distribution for the large magnitudes and an exponential distribution for the smaller size earthquakes. The uniform distribution is centered on the mean characteristic magnitude and has a width of 0.5 magnitude. Since this model is a composite of two distributions, an additional constraint is needed to define the relative amplitudes of the two distributions. This is done by setting the height of the uniform distribution to be equal to the value of the exponential distribution at 1.0 magnitude units below the lower end of the characteristic part (1 magnitude unit less

than the lower magnitude of the uniform distribution). This additional constraint sounds rather arbitrary, but it has an empirical basis. The key feature is that this constraint results in about 94% of the total seismic moment being released in characteristic earthquakes and about 6% of the moment being released in the smaller earthquakes that fall on the exponential tail. Other forms of the model could be developed (e.g. a uniform distribution with a width of 0.3 magnitude units). As long as the fractional contribution of the total moment remains the same, then the hazard is not sensitive to there details.

The equations for the magnitude density function for the Youngs and Coppersmith characteristic model are given by

$$f_m^{YC}(m) = \begin{cases} \dfrac{1}{1+c_2}\,\dfrac{\beta\exp(-\beta(\overline{M}_{char}-M_{\min}-1.25)}{1-\exp(-\beta(\overline{M}_{char}-M_{\min}-0.25)} & for\ \ \overline{M}_{char}-0.25 < M \le \overline{M}_{char}+0.25 \\ \dfrac{1}{1+c_2}\,\dfrac{\beta\exp(-\beta(M-M_{\min})}{1-\exp(-\beta(\overline{M}_{char}-M_{\min}-0.25)} & for\ \ M_{\min} \le M \le \overline{M}_{char}-0.25 \end{cases} \quad (6.19)$$

where

$$c_2 = \frac{0.5\beta\exp(-\beta(\overline{M}_{char}-M_{\min}-1.25)}{1-\exp(-\beta(M_{char}-M_{\min}-0.25)} \quad (6.20)$$

6.6 Activity Rates

The magnitude density functions described in section 6.5 above give the relative rate of different earthquake magnitudes on a source (above some given minimum magnitude). To compute the absolute rate of earthquakes of different magnitudes requires an estimate of rate of earthquakes above the minimum magnitude, which is called the activity rate and is denoted $N(M_{min})$.

There are two common approaches used for estimating the activity rates of seismic sources: historical seismicity and geologic (and geodetic) information.

6.6.1 Activity Rate Based on Historic Seismicity

If historical seismicity catalogs are used to compute the activity rate, then the estimate of $N(M_{min})$ is usually based on fitting the truncated exponential model to the historical data from an earthquake catalog. When working with earthquake catalogs, there are several important aspects to consider: magnitude scale, dependent events, and completeness.

The catalog needs to be for a single magnitude scale. Typically, historical earthquakes will be converted to moment magnitude as discussed previously.

Dependent events, aftershocks and foreshocks, need to be removed from the catalog. The probability models that are used for earthquake ocurrence assume that the earthquakes are independent. Clearly, aftershocks and foreshocks are dependent and do not satisfy this assumption. The definition of what is an aftershock and what is a new earthquake sequence is not simple. It is most common for the dependent earthquakes to be idenified by a magnitude dependent time and space window. Any earthquake that fall with a specified time or distance from an earthquake (and has a smaller magnitude) is defined as an aftershock. The size of the time and space windows can vary from region to region, but in all cases the window lengths are greater for larger magnitude earthquakes.

Once the catalog has been converted to a common magnitude scale and the dependen evens have been removed, the catalog is then evaluated for completeness. Figure 6-7 shows an evaulation of the completeness for the Swiss earthquake catalog.

The model of the activity rate from historical catalogs assumes that all events the occurred in the time period covered by the catalog have been reported in the catalog. In general, this is not the case and the catalogs are incomplete for the smaller magnitudes. A method for evaluating catalog completeness was developed by Stepp (1972). In this method, the rate of earthquakes is plotted as a function of time, starting at the present and moving back toward the beginning of the catalog. If the occurrence of earthquakes is stationary (not changing with time), then this rate should be approximately constant with time. If the catalog is incomplete, then the rate should start to decline. This process is used to estimate the time periods of completeness for

specific magnitude ranges. An example is shown in Figure 6-7 for the Swiss catalog. In this example, the magnitude 6 and larger earthquakes are complete for about 400 years, but the magnitude 3 earthquakes are complete for about 150 years. The rate of each magnitude is computed over the time period for which it is complete.

Once the catalog has been corrected for completeness, the b-value and the activity rate are usually computed using the maximum likelihood method (Weicherdt, 1980) rather han least-squares fit to the cumulative rate. The maximum likelihood estimate for the b-value is given by

$$b = \frac{1}{\ln(10)\left(\overline{M} - M_{\min}\right)} \qquad (6\text{-}21)$$

and the activity rate is simple the observed rate at the minimum magnitude.

The maximum likelihood method is generally preferred because the cumulative rate data are not independent and least-squares gives higher weight to rare large magnitude events that may not give a reliable long term rate. As an example, an artificial data set was generated using the truncated expontial distribution with a b-value of 1.0. This sample was then fit using maximum likelihood and using least-squares. As shown in Figure 6-8, the least-sqaures fit lead to a b-value much smaller than the population sampled (b=1.0). In this example, the maximum likelihood method gives a b-value of 0.97, but the least-squares model gives a b-value of 0.68. The use of the maximum likelihood method, depends on quality of the catalog at the smallest magnitudes used.

Typical b-values are between 0.8 and 1.2 for crustal sources. For subduction zones, lower b-values (0.5 – 1.0) are common. If the b-value is outside of this range, then they should be reviewed for possible errors such as not removing dependent events, not accounting for catalog completeness, and the fitting method (e.g. use of odrinary least-squares to fit the cumulaive data).

6.6.2 Activity Rate based on Slip-Rate

If fault slip-rate is used to compute the activity rate, then the activity rate is usually computed by balancing the long-term accumulation of seismic moment with the long-term release of seismic moment in earthquakes.

The build up of seismic moment is computed from the long-term slip-rate and the fault area. The annual rate of build up of seismic moment is given by the time derivative of eq. (6.1):

$$\frac{dM_o}{dt} = \mu A \frac{dD}{dt} = \mu A S \qquad (6.22)$$

where S is the fault slip-rate in cm/year. The seismic moment released during an earthquake of magnitude M is given by eq. (6.3).

The slip-rate is converted to an earthquake activity rate by requiring the fault to be in equilibrium. The long-term rate of seismic moment accumulation is set equal to the long-term rate of the seismic moment release. The activity rate of the fault will depend on the distribution of magnitudes of earthquakes that release the seismic energy. For example, a fault could be in equilibrium by releasing the seismic moment in many moderate magnitude earthquakes or in a few large magnitude earthquakes. The relative rate of moderate to large magnitude earthquakes is described by the magnitude pdfs that were described in section 6.5.

As an example of the method, consider a case in which only one size earthquake occurs on the fault. Assume that the fault has a length of 100 km and a width of 12 km and a slip-rate of 5 mm/yr. The rate of moment accumulation is computed using eq. (6-21)

$$\mu AS = (3 \times 10^{11} \text{ dyne/cm}^2)\ (1000 \times 10^{10} \text{ cm}^2)\ (0.5 \text{ cm/yr})$$
$$= 1.5 \times 10^{24} \text{ dyne-cm/yr}$$

Next, using the simplified magnitude-area relation (eq. 6-13), the mean magnitude is

$M = \log(1000) + 4 = 7.0,$

and the moment for each earthquake is

$$M_o/eqk = 10^{(1.5x7.0+16.05)} = 3.5 \times 10^{26} \text{ dyne-cm/eqk}$$

The rate of earthquakes, N, is the ratio of the moment accumulation rate to the moment released in each earthquake

$$N = \frac{\mu AS}{M_o/eqk} = \frac{1.5x10^{24}\ dyne-cm/yr}{3.5x10^{27}\ dyne-cm/eqk} = 0.0043\ eqk/yr$$

This approach can be easily generalized to an arbitrary form of the magnitude pdf. The rate of earthquakes above some specified minimum magnitude, $N(M_{min})$, is given by the ratio of the rate of accumulation of seismic moment to the mean moment per earthquake with $M>M_{min}$. From Chapter 4 (eq. 4.10), the mean moment per earthquake is given by

$$Mean\left[\frac{M_o}{eqk}\right] = \int_{m\,\min}^{M\,\max} 10^{(1.5M+16.05)} f_m(M)\,dM \qquad (6\text{-}23)$$

and the activity rate is given by

$$N(M_{\min}) = \frac{\mu AS}{Mean[M_o/eqk]} \qquad (6\text{-}24)$$

6.7 Magnitude Recurrence Relations

Together, the magnitude distribution and the activity rate are used to define the magnitude recurrence relation. The magnitude recurrence relation, N(M), describes the rate at which earthquakes with magnitudes greater than or equal to M occur on a source (or a region). The recurrence relation is computed by integrating the magnitude density function and scaling by the activity rate:

$$N(M) = N(M_{\min}) \int_{m=M}^{M_{\max}} f_m(m)\,dm$$

(6-25)

Although the density functions for the truncated exponential and Y&C characteristic models are similar at small magnitudes (Figure 6-5), if the geologic moment-rate is used to set the annual rate of events, $N(M_{min})$, then there is a large impact on the computed activity rate depending on the selection of the magnitude density function. Figure 6-9 shows the comparison of the magnitude recurrence relations for the alternative magnitude density functions when they are constrained to have the same total moment rate. The characteristic model has many fewer moderate magnitude events than the truncated exponential model (about a factor of 5 difference). The maximum magnitude model does not include moderate magnitude earthquakes. With this model, moderate magnitude earthquakes are generally considered using areal source zones.

The large difference in the recurrence rates of moderate magnitude earthquakes between the Y+C and truncated exponential models can be used to test the models against observations for some faults. The truncated exponential model significantly overestimates the number of moderate magnitude earthquakes. This discrepancy can be removed by increasing the maximum magnitude for the exponential model by about 1 magnitude unit. While this approach will satisfy the both the observed rates of moderate magnitude earthquakes and the geologically determined moment rate, it generally leads to unrealistically large maximum magnitudes for known fault segments (e.g. about 4-6 standard deviations above the mean from a magnitude-area scaling relation) or it requires combining segments of different faults into one huge rupture. Although the truncated exponential model does not work well for faults in which the geologic moment-rate is used to define the earthquake activity rate, in practice it is usually still included as a viable model in a logic tree because of it wide use in the past. Including the truncated exponential model is generally conservative for high frequency ground motion (f>5 hz) and unconservative for long period ground motions (T>2 seconds).

6.8 Rupture Location Density Functions

The final part of the source characterization is the distribution of the locations of the ruptures. For faults, a uniform distribution along the strike of the fault plane is

commonly used and a triangle distribution or lognormal distribution is often used for the location down-dip.

For areal sources, the earthquakes are typically distributed uniformly with a zone (in map view) and a triangle distribution or lognormal distribution is often used for the location at depth. For the areal source zone that contains the site, it is important that a small integration step size for the location pdf be used so that the probability of an earthquake being located at a short distance from the site is accurately computed. The step size for the zone containing the site should be no greater than 1 km.

6.9 Earthquake Probabilities

The activity rate and the magnitude pdf can be used to compute the rate of earthquake with a given magnitude range. To convert this rate of earthquakes to a probability of an earthquake requires an assumption of earthquake occurrence. Two common assumptions used in seismic hazard analysis are the Poisson assumption and the renewal model assumption.

6.9.1 Poisson Assumption

A standard assumption is that the occurrence of earthquakes is a Poisson process. That is, there is no memory of past earthquakes, so the chance of an earthquake occurring in a given year does not depend on how long it has been since the last earthquake. For a Poisson process, the probability of at least one occurrence of an earthquake above M_{min} in t years is given by eq. 4.28:

$$P(M>M_{min}|t) = 1 - \exp(-\nu(M> M_{min})t) \qquad (6.26)$$

In PSHA, we are concerned with the occurrence of ground motion at a site, not the occurrence of earthquakes. If the occurrence of earthquakes is a Poisson process then the occurrence of peak ground motions is also a Poisson process.

6.9.2 Renewal Assumption

While the most common assumption is that the occurrence of earthquakes is a Poisson process, an alternative model that is often used is the renewal model. In the renewal model, the occurrence of large earthquakes is assumed to have some periodicity. The conditional probability that an earthquake occurs in the next ΔT years given that it has not occurred in the last T years is given by (7)

$$P(T,\Delta T)=\frac{\int_{T}^{T+\Delta T} f(t)\,dt}{\int_{T}^{\infty} f(t)\,dt}$$

where f(t) is the probability density function for the earthquake recurrence intervals. Several difference forms of the distribution of earthquake recurrence intervals have been used: normal, log-normal, Weibull, and Gamma. In engineering practice, the

most commonly used distribution is the log-normal distribution. The lognormal distribution is given by (eq. 4-19):

$$f^{LN}(t)=\frac{1}{\sqrt{2\pi}\sigma_{\ln t}t}\exp\frac{-(\ln(t)-\ln(\mu))^2}{2\sigma_{\ln t}^2} \tag{6.28}$$

Although lognormal distributions are usually parameterized by the median and standard deviation, in renewal models, the usual approach is to parameterize the distribution by the mean and the coefficient of variation (C.V.). For a log normal distribution, the relations between the mean and the median, and between the standard deviation and the C.V. are given in eq. 4.20 and 4.21:

$$\mu=\frac{\overline{T}}{\exp(\sigma_{\ln t}^2/2)} \tag{6.29}$$

$$\sigma_{\ln t}=\sqrt{\ln(1+CV^2)} \tag{6.30}$$

The conditional probability computed using the renewal model with a lognormal distribution is shown graphically in Figure 6-10. In this example, the mean recurrence interval is 200 years and the coefficient of variation (C.V.) is 0.5. The conditional probability is computed for an exposure time of 50 years assuming that it has been 200 years since the last earthquake. Graphically, the conditional probability is given by the ratio of the area labeled "A" to the sum of the areas labeled "A" and "B". That is, P(T=200,ΔT=50)=A/(A+B).

An important parameter in the renewal model is the C.V.. The C.V. is a measure of the periodicity of the earthquake recurrence intervals. A small C.V. (e.g. C.V. < 0.3) indicates that the earthquakes are very periodic, whereas a large C.V. (e.g. C.V>>1) indicates that the earthquakes are not periodic. Early estimates of the C.V. found small C.V. of about 0.2 (e.g. Nishenko, 1982); however, more recent estimates of the C.V. are much larger, with C.V. values ranging from 0.3 to 0.7. In practice, the typical C.V. used in seismic hazard analysis between 0.4 and 0.6. The sensitivity of the conditional probability to the C.V. is shown in Figures 6-11 and 6-12 for a 50 and 5

year exposure periods, respectively. For comparison, the Poisson rate is also shown. These figures shows that the renewal model leads to higher probabilities once the elapse time since the last earthquake is greater than about one-half of the mean recurrence interval. In addition, these figures show that as the C.V. becomes larger, the conditional probability becomes closer to the Poisson probability.

Figures 6-11 and 6-12 show one short-coming of the lognormal distribution when applied to the renewal model. As the time since the last earthquakes increases past about twice the mean recurrence interval, the computed probability begins to decrease, contrary to the basic concept of the renewal model that the probability goes up as the time since the last earthquake increases (e.g. strain continues to build on the fault).

To address this short-coming of the lognormal model, Mathews (1999) developed a new pdf for earthquake recurrence times called the Brownian Passsage Time (BPT) model. The pdf for this model is given by:

$$f_{\tau}^{BPT}(\tau, CV, \overline{T}) = \frac{1}{2\pi CV^2 \tau^3} \exp\left(-\ln(\tau) - \frac{\overline{T}}{\Delta T}\right)$$

where τ is the normalized time since the last event:

$$\tau = \frac{t}{\overline{T}}$$

The pdf for the lognormal and BPT model are compared in Figure 6-13 for a CV=0.5 and a mean recurrence interval of 200 years. These two pdfs are very similar. The difference is that the BPT model puts more mass in the pdf at large recurrence times that avoids the problem of the probability reducing for large recurrence times. This increase in mass at large recurrence times is shown in Figure 6-14 which is a blow-up of the pdf shown in Figure 6-13.

Another difference between the lognormal and BPT models is a very short recurrence times. At short recurrence times, the BPT model has less mass than the lognormal

model as shown in Figure 6-15. This will lead to lower earthquake probabilities shortly after a large earthquake occurs.

The probabilities computed using the lognormal and BPT models are shown in Figure 6-16 for a mean recurrence of 200 years and a CV of 0.5. This figure shows that the BPT model is very similar to the lognormal model, but does not have the undesirable feature or decreasing probabilities for long recurrence times. For this reason, the BPT model is preferred over the log-normal model.

Importance of Assessing Degrees of Fault Activity for Engineering Decisions
Cluff, L.S., and J.L.Cluff

As published in

"*Proceeding of the 8th World Conference on Earthquake Engineering,*"
Vol. 2, Prentice-Hall, Englewood Cliffs, N.J., pp. 629–636, (1984)

IMPORTANCE OF ASSESSING DEGREES OF FAULT ACTIVITY FOR ENGINEERING DECISIONS

L. S. Cluff (I)
J. L. Cluff (I)
Presenting Author: L. S. Cluff

SUMMARY

Classifying faults as either "active" or "inactive" is a scientific oversimplification that usually results in overconservatism in the siting and design of structures. Because of the need to more accurately define the range in the degree of activity of faults, the behavioral characteristics of more than 150 active faults worldwide were compared. The faults were found to differ by several orders of magnitude in many of their characteristics, especially in rates of slip and in size and frequency of earthquakes. A classification scheme has been developed using six different activity classifications to provide a more realistic framework for seismic hazard and risk assessments.

INTRODUCTION

Decisions with regard to seismic safety for many critical facilities have become legal battles in which opponents to the facility grasp the earthquake issue as an excuse to invalidate the facility or the chosen site, and, in defense, site advocates often tend to understate the earthquake issues. In many cases, the seismic safety decision process has consumed years, has cost millions of dollars, and has become a disservice to society.

A major factor that has confused nontechnical decision makers is that earthquake hazards have been characterized by classifying faults as either "active" or "inactive" based soley on the recency of fault displacement. This has led to rigid legal definitions of fault activity based on a specified time criterion. For example, the U.S. Nuclear Regulatory Commission considers a fault active if it has evidence of multiple displacements in 500,000 years, or evidence of a single displacement in 35,000 years. For the purpose of classifying faults at sites of major dams, the U.S. Bureau of Reclamation has used 100,000 years, and the U.S. Army Corps of Engineers has used 35,000 years as their criteria for time intervals since the most recent fault displacement. Once a fault is classified as active by applying these criteria, it is considered equal to other active faults from a legal point of view. This is a scientific oversimplification and usually results in unrealistic overconservatism in the siting and design of structures.

(I) Woodward-Clyde Consultants, Walnut Creek, California, USA

Realistic earthquake hazard assessments and risk analyses must recognize the differences that exist in the degree to which faults are active. Because of the need to more accurately define the range in degree of activity of faults to provide a more satisfactory framework for seismic hazard and risk assessments by decision-makers, a classification scheme that considers the different factors that cause variations in fault activity has been developed. Using this degree of fault activity classification scheme should result in a more realistic, technical basis for seismic safety decisions.

FAULT ACTIVITY CHARACTERISTICS

Significant differences exist in the degree to which various faults are active. The differences in relative degree of activity are manifested by several fault behavioral characteristics, including rate of strain release or fault slip, amount of fault displacement in each event, length of fault rupture, earthquake size, and earthquake recurrence interval. These behavioral characteristics are a function of the tectonic environment, the fault type and geometry, the rate of strain accumulation, the direction of crustal stress, the stratigraphic character and physical properties of the earth's crust, and the complexity and physical properties of the fault zone.

Slip Rate

The geologic slip rate provides a measure of the average rate of deformation across a fault. The slip rate is calculated by dividing the amount of cumulative displacement, measured from displaced geologic or geomorphic features, by the age of the geologic material or feature. The geologic slip rate is an average value through the geologic time period being considered, and reliable to the extent that strain accumulation and release over the time period has been uniform and responding to the same tectonic stress environment. In some tectonic environments, the current stress conditions have only been in effect for about 1.5 million years; in others, the stress conditions have been in force for 4 to 5 million years, or even for more than 10 million years. Many faults, particularly the highly active ones, displace multiple markers of different ages, allowing comparisons of slip rates through time.

Slip Per Event

The amount of fault displacement for each fault rupture event differs among faults and fault segments and provides another indication of relative differences in degrees of fault activity. The differences in amounts of displacement are governed by the tectonic environment, fault type and geometry and pattern of faulting, and the amount of accumulated strain being released.

The amount of slip per event can be directly measured in the field during studies of historical faulting, and is usually reported in maximum and average values. Displacements for prehistoric rupture

events can be estimated for some faults from detailed surface and subsurface seismic geologic investigation (for example, Ref. 1, 2).

It is often difficult to decide what value is most accurate and representative of maximum or average displacements from data available in the literature. Often, reported displacement values represent apparent displacement or separation across a fault. For normal faulting events, scarp height has typically been reported as a measurement of the tectonic displacement. The scarp height, however, often exceeds the net tectonic displacement across a fault by as much as two times, due to graben formation and other effects near the fault (Ref. 2). In the case of thrust faults, the reported vertical displacement often is actually the measure of vertical separation, and the net slip on the fault has been underestimated by a significant amount.

Rupture Length

The length of the fault rupture significantly influences the size of the resulting earthquakes. It is mechanically not possible for a large earthquake to be released along a fault of short length, and, from worldwide data of historical earthquakes, a rough correlation exists between fault rupture length and earthquake magnitude (Ref. 3).

Earthquake Size

The earliest measures of earthquake size were based on the maximum intensity and areal extent of perceptible ground shaking. Instrumental recordings of ground shaking led to the development of the magnitude scale. Although the scale permitted quantitative comparisons of earthquake size, magnitude was defined empirically from the amplitudes of seismic waves, and the "size" that it measured was not definable in terms of any aspect of the physical process of faulting. In defining seismic moment, theoretical seismology has provided a physically meaningful measure of the size of a faulting event. Seismic moment is related directly to the static parameters of an earthquake, including shear modulus, average fault displacement, and the rupture area.

The magnitude value is a good estimate of earthquake size to the extent that the period of the wave used is longer than the rupture duration of the earthquake. The surface-wave magnitude scale, M_s, uses 20-second-period surface waves, and saturates at $M_s = 7.5$. That is, the amplitudes of 20-second-period surface waves stop increasing linearly with magnitude at $M_s = 7.5$, and become insensitive to further increases in earthquake size. Thus, earthquake size is not accurately reflected by the M_s measurement when earthquake size exceeds $M_s = 7.5$. Local magnitude, M_L, and body wave magnitude, m_b, use shorter period waves and thus saturate at even lower magnitudes.

Hanks and Kanamori (Ref. 4) have proposed a moment-magnitude scale, M, in which magnitude is calculated from seismic moment using an empirical formula. The moment-magnitude scale does not saturate, because it is based on seismic moment, a true measure of the size of an

earthquake. Moment magnitude is well calibrated with the M_w scale of Kanamori (Ref. 5), which is a theoretically based moment-magnitude scale, and with M_s and M_L below their respective saturation levels.

The use of magnitude or seismic moment as a criterion for the comparison of fault activity requires the choice of the magnitude or moment value that is characteristic of the fault. Of course, in many instances it is not possible to ascertain whether historical seismic activity is characteristic of the fault through geologic time, unless a long historical seismic record is available or evidence of the sizes of past earthquakes is available from seismic geology studies of paleoseismicity. In a few cases, detailed seismic geology studies have yielded data on the sizes of past surface faulting earthquakes (Ref. 1, 2). In general, these data involve measurements of prehistoric rupture length and/or displacement, and a seismic moment or magnitude can be estimated probably within one-half magnitude.

Recurrence Interval

Faults having different degrees of activity differ by several orders of magnitude in the average recurrence intervals of significant earthquakes. Comparisons of recurrence provide a useful means of assessing the relative activity of faults, because the recurrence interval provides a direct link between slip rate and earthquake size. Recurrence intervals can be calculated directly from slip-rate and displacement-per-event data. In some cases, where the record of historical seismicity is sufficiently long compared to the average recurrence interval, seismicity data can be incorporated when estimating recurrence. In many regions of the world, however, the historical seismicity record is too brief; some active faults have little or no historical seismicity and the recurrence time between significant earthquakes is longer than the available historical record along the fault of interest. Plots of frequency of occurrence versus magnitude can be prepared for small to moderate earthquakes and extrapolations to larger magnitudes can provide estimates of the mean rate of occurrence (b-values) of larger magnitude earthquakes. This technique has limitations, however, because it is based on regional seismicity, and cannot result in reliable recurrence intervals for specific faults.

CLASSIFICATION SCHEME

The behavioral characteristics of more than 350 active faults worldwide were researched for analysis. Particular emphasis was placed on examining data from faults that have experienced historical surface displacement, because data were expected to be available for most fault activity characteristics. One hundred fifty faults were chosen to represent all styles of faulting within different tectonic environments around the world. Data were obtained on the various activity characteristics of these faults, and order-of-magnitude differences were recognized. Cluff and others (Ref. 6) show classes of active faults established based on patterns of combinations of characteristics (Table 1).

TABLE

FAULT CLASSIFICA

CLASS 1

Slip Rate ≥ 10 mm/yr
Slip per Event ≥ 1 m
Rupture Length ≥ 100 kr
Seismic Moment ≥ 10^{26} (
Magnitude ≥ M_s 7.5
Recurrence Interval < 50

CLASS 1A

Same as Class 1.
Slip Rate ≥ 5 m
Recurrence Inte

CLASS 1B

Same as Class 1.
Slip per Event <
Magnitude < M
Recurrence Inte

CLASS 2

Slip Rate: 1-10 mm/yr
Slip per Event ≥ 1 m
Rupture Length 50-20
Seismic Moment ≥ 10^{2}
Magnitude ≥ M_s 7.0
Recurrence Interval 10

CLASS 2A

Same as Class 2
Slip per Event
Magnitude < M
Short I<100 y

CLASS 2B

Same as Class
Slip per Event
Rupture Lengt
Recurrence In

CLASS 3

Slip Rate: 0.5-5 mm/y
Slip per Event: 0.1-3 n
Rupture Length: 10-1
Seismic Moment ≥ 10
Magnitude ≥ M_s 6.5
Recurrence Interval 5

CLASS 4

Slip Rate: 0.1-1 mm/
Slip per Event: 0.01-1
Rupture Length 1-5C
Seismic Moment ≥ 10
Magnitude ≥ M_s 5.5
Recurrence Interval 1

CLASS 4A

Same as Class
Slip per Even
Rupture Len
Seismic Mom
Magnitude ≥

CLASS 5

Slip Rate < 1mm/yr
Recurrence Interval

CLASS 6

Slip Rate < 0.1 mm/
Recurrence Interval

TABLE 1

FAULT CLASSIFICATION CRITERIA

CLASS 1

Slip Rate ≥ 10 mm/yr
Slip per Event ≥ 1 m
Rupture Length ≥ 100 km
Seismic Moment ≥ 10^{26} dyne-cm
Magnitude ≥ M_s 7.5
Recurrence Interval ≤ 500 yrs

CLASS 1A

Same as Class 1, except:
Slip Rate ≥ 5 mm/yr
Recurrence Interval ≤ 1000 yrs

CLASS 1B

Same as Class 1, except:
Slip per Event < 1 m
Magnitude < M_s 7.0
Recurrence Interval generally ≤ 100 yrs

CLASS 2

Slip Rate: 1-10 mm/yr
Slip per Event ≥ 1 m
Rupture Length: 50-200 km
Seismic Moment ≥ 10^{25} dyne-cm
Magnitude ≥ M_s 7.0
Recurrence Interval: 100-1000 yrs

CLASS 2A

Same as Class 2, except:
Slip per Event < 1 m
Magnitude < M_s 7.0
Short (<100 yrs) Recurrence Interval

CLASS 2B

Same as Class 2, except
Slip per Event ≥ 5 m
Rupture Length ≥ 100 km
Recurrence Interval ≥ 1000 yrs

CLASS 3

Slip Rate: 0.5-5 mm/yr
Slip per Event: 0.1-3 m
Rupture Length: 10-100 km
Seismic Moment ≥ 10^{25} dyne-cm
Magnitude ≥ M_s 6.5
Recurrence Interval: 500-5000 yrs

CLASS 4

Slip Rate: 0.1-1 mm/yr
Slip per Event: 0.01-1 m
Rupture Length: 1-50 km
Seismic Moment ≥ 10^{24} dyne-cm
Magnitude ≥ M_s 5.5
Recurrence Interval: 1000-10,000 yrs

CLASS 4A

Same as Class 4, except:
Slip per Event ≥ 0.5 m
Rupture Length ≥ 10 km
Seismic Moment ≥ 10^{25} dyne-cm
Magnitude ≥ M_s 6.5

CLASS 5

Slip Rate < 1mm/yr
Recurrence Interval ≥ 10,000 yrs

CLASS 6

Slip Rate < 0.1 mm/yr
Recurrence Interval ≥ 100,000 yrs

Six general classes of active faults and five sub-clases have been identified. The sub-classes have most of the same characteristics as the larger classes, but important differences in fault behavior necessitated sub-class designations. A brief discussion of several faults will illustrate the classification scheme.

The south-central segment of the San Andreas fault, from Cholame to San Bernardino in southern California, can be considered a Class 1 fault. A geologic slip rate of about 40 mm/yr has been calculated for Holocene displacement along the fault. Recurrence intervals ranging from about 100 to 330 years have been estimated for great earthquakes similar to the 1857 event (M 8) that produced up to 9.5 m of right slip. The Parkfield segment of the San Andreas fault is Class 1B because, although the slip rate is similar to that of the south-central segment, the magnitude (less than M_s 6.5), displacement (less than 0.5 to 1.0 m), and recurrence interval (less than 30 years) of historical earthquakes are much different. Available evidence indicates that such behavior --frequent small rupture events--is characteristic of this segment, whereas less frequent, large rupture events characterize the adjacent south-central segment.

The Motagua fault of Guatemala, source of the 1976 M_s 7.5 earthquake, is typical of the larger faults of Class 2. The late Quaternary slip rate is about 6 mm/yr, typical rupture events produce about 1 to 2 m of right slip, and recurrence intervals of around 200 years appear to be characteristic. Somewhat less active strike-slip faults, such as the Calaveras and Hayward faults in northern California, are also included in Class 2. The Wasatch fault of Utah is a good example of a Class 2 intraplate normal fault: slip rate is

about 1.5 mm/yr, displacement per event is 1 to 3 m, recurrence intervals along individual segments range from 500 to 2500 years, and are probably less than 500 years for the entire fault.

The Elsinore fault in southern California is a typical Class 3 strike-slip fault: slip rate is about 3 mm/yr, slip events are relatively small, and recurrence intervals are moderately long, up to a few thousand years. The Sierra Madre fault, source of the 1971 San Fernando earthquake, illustrates Class 3 reverse faulting: slip rate is 1 to 2 mm/yr and recurrence intervals range from a few to several thousands of years. Many Basin and Range normal faults fall into Class 3, including the Dixie Valley and Pleasant Valley faults.

Many Class 4 faults have been recognized. The Greenville fault in northern California is typical: slip rate is probably less than 0.5 mm/yr; minor surface faulting was associated with an earthquake of magnitude less than 6. Most of the reverse faults of the Transverse Range of California are in Class 4; their slip rates generally are 0.2 to 0.8 mm/yr. Class 4A is an important sub-class. It represents a group of faults having relatively low slip rates, large-magnitude earthquakes, and relatively long recurrence intervals. For example, the Zenkoji fault in Japan has a slip rate of less than 0.2 mm/yr, yet produced an estimated M_s 7.4 earthquake in 1847.

Faults of Class 5, and especially Class 6, generally behave similarly to faults of Class 4A: low slip rates are accompanied by large earthquakes having very long recurrence intervals. The most dramatic example is the Pitaycachi fault, source of the 1887 Sonora, Mexico, earthquake. The slip rate appears to be only about 0.02 mm/yr, yet an estimated M_L 7.5 earthquake in 1887 was accompanied by as much as 4 m of normal fault displacement. Geomorphic studies of the fault zone suggest a hiatus of several hundred thousand years between periods of fault displacement.

The principal advantage of this degree of activity fault classification scheme is that all the characteristics that can be used to define fault behavioral activity are incorporated, thus, this scheme incorporates the range of fault behavior. In using this classification, if certain characteristics of a fault are known, then relatively restricted values for other characteristics of the fault can be calculated or deduced.

During the analysis of fault activity data, it was quickly recognized that faults do not behave in simple order-of-magnitude classifications. Significant overlap is recognized among various characteristics. A fault that has a slip rate of 0.7 mm/yr and a recurrence interval of 2000 years of a 0.5 m displacement might fit either Class 3 or Class 4. The Rose Canyon and the La Nacion faults near San Diego, California, would be Class 5 with regard to recurrence interval, and Class 6 with regard to slip rate. The choice of a particular classification will depend on the preponderance of evidence

of fault activi
appropriate to

Seismic ge
electric projec
seismic hazard
can assist deci
critical struct
where earthqual
seismic hazard
project planned
Interconexion I
companies for (
several of the:

It was fo
Colombia could
regional tecto
sive investiga
potential for
considered to
Further detail
slip rates and
originally est
incorrectly lo
activity to co
into considera
reassessed as
made between a
in the design
of the seismic

The resul
to quantitativ
possible hazar
likelihood of
to be 1000 to
entering the r
evaluation and

In Califo
became so ent
rose to $400 r
eventually re
scientific an
the site-appr
evaluated. T
and were deve
controversial

of fault activity; where two options are available, it is generally appropriate to choose the class having the higher degree of activity.

VALUE IN SEISMIC HAZARD ASSESSMENTS

Seismic geology and seismicity studies for more than ten hydroelectric projects in Colombia, South America provide examples of how seismic hazard evaluations using the degree of fault activity concept can assist decision-makers in making assessments of relative risk to critical structures. Because Colombia is a tectonically active region where earthquakes are relatively common, prudence dictated that detailed seismic hazard evaluations be performed for every major hydroelectric project planned. Many of these studies have been conducted by Interconexion Electrica S.A. (ISA), the central consortium of power companies for Colombia, and their consultants for the past 10 years, and several of these projects are now being designed and constructed.

It was found that the degree of fault activity on faults in Colombia could be reassessed based on the increased understanding of regional tectonics and Quaternary faulting rates gained during successive investigations. Faults considered active because they have the potential for slip in the current tectonic stress regime were first considered to have a moderate to high degree of activity (Class 1). Further detailed seismic geologic and seismicity studies showed that the slip rates and amounts of displacement on some faults were less than originally estimated, and several large historical earthquakes were incorrectly located. Not having a rigid, legal definition of fault activity to constrain decision-makers allowed this new data to be taken into consideration. The degree of fault activity on these faults was reassessed as low to moderate (Class 3). As a result, choices could be made between alternate sites, and significant savings are being realized in the design and construction of major projects where such assessments of the seismic hazard can be made with confidence.

The results of the seismic hazard studies also provided a mechanism to quantitatively compare the hazard from faulting with the other possible hazards. For example, at one dam site in Colombia, the likelihood of surface fault rupture through the dam foundation was found to be 1000 to 10,000 times less than the likelihood of a large landslide entering the reservoir. This information aided decision-makers in the evaluation and selection of the type of dam for this site.

In California, the siting of a liquefied natural gas (LNG) terminal became so entangled in debates over seismic safety that the project cost rose to $400 million prior to facility design, and the extensive delays eventually resulted in cancellation of the project. Although many scientific and environmental issues were the subjects of debate during the site-approval phases of this project, most of them could be easily evaluated. The seismic safety issues, however, were more complicated and were developed into major obstacles to the siting of this controversial facility.

Fault activity was defined in such a way that the seismic issues could be and were misused. One major stumbling block in the decision process was a legalistic definition of fault activity based on a specific time criterion: faults older than 100,000 to 140,000 years were "safe;" younger ones were not. The criteria also included the term "maximum credible earthquake." Use of this term invites controversy, because what it credible to one person may not be credible to another.

The LNG case was finally resolved by engaging a panel of experts, who shunned the previously adopted criteria and terminology (Ref. 7). The panel addressed the "active fault" problem by describing the earthquake sources important to the proposed LNG terminal site according to their degree of activity. This involved estimating earthquake magnitudes for various recurrence intervals for each earthquake source. Instead of "maximum credible earthquake," the panel recommended that likely maximum earthquakes for different recurrence intervals be considered when choosing design parameters. This approach allows choices to be made that are consistent with judgments about acceptable risk.

4.7 The

REFERENCES

1. Sieh, K.E., 1978, Prehistoric large earthquakes produced by slip on the San Andreas fault at Pallett Creek, California: Journal of Geophysical Research, v. 83, no. B8, p. 3907-3939.

2. Swan, F.H., III, Schwartz, D.P., and Cluff, L.S., 1980, Recurrence of moderate to large magnitude earthquakes produced by surface faulting on the Wasatch fault zone, Utah: Bulletin of the Seismological Society of America, v. 70, no. 5, p. 1431-1462.

3. Slemmons, D.B., 1977, State-of-the-art for assessing earthquake hazards in the United States; Report 6, faults and earthquake magnitude: U. S. Army Corps of Engineers, Waterways Experiment Station, Soils and Pavements Laboratory, Vicksburg, Mississippi, Miscellaneous Paper S-73-1, 129 p.

4. Hanks, T.C., and Kanamori, H., 1979, A moment magnitude scale: Journal of Geophysical Research, v. 84, no. 20, p. 2981-2987.

5. Kanamori, H., 1977, The energy release in great earthquakes: Journal of Geophysical Research, v. 82, p. 2981-2987.

6. Cluff, L.S., Coppersmith, K.J., and Knuepfer, P.L., 1982, Assessing degrees of fault activity for seismic microzonation: Third International Earthquake Microzonation Conference Proceedings, v. 1, p. 113-118.

7. Cluff, L.S., Chairman, LNG Seismic Review Panel, 1981, Seismic Safety Review of the Proposed Liquefied Natural Gas Facility, Little Cojo Bay, Santa Barbara County, California: unpublished report for the California Public Utilities Commission, 33 p.